ELSEVIER

Chemical Geology 172 (2001) 225–250

CHEMICAL GEOLOGY
INCLUDING
ISOTOPE GEOSCIENCE

www.elsevier.com/locate/chemgeo

Dissolution of primary minerals of basalt in natural waters I. Calculation of mineral solubilities from 0°C to 350°C

Andri Stefánsson *

Science Institute, University of Iceland, Dunhagi 3, 107 Reykjavik, Iceland

Received 24 July 1998; accepted 4 April 2000

Abstract

The solubilities of forsterite, fayalite, enstatite, ferrosilite, hedenbergite, diopside, anorthite, high-albite, magnetite, hematite, ulvöspinel, ilmenite, F-apatite and OH-apatite and olivine, plagioclase, orthopyroxene, clinopyroxene and Fe–Ti oxide solid solutions of fixed composition were calculated in the temperature range 0–350°C at saturated water vapour pressure. The thermodynamic database used for end-member minerals was that of Robie and Hemingway [Robie, R.A., Hemingway, B.S., 1995. Thermodynamic properties of minerals and related substances at 298.15 K and 1 bar (105 Pascals) pressures and at higher temperatures. U.S. Geol. Surv. Bull. 2131, 461 pp.] except for plagioclases [Arnórsson, S., Stefánsson, A., 1999. Assessment of feldspar solubility constants in water in the range of 0° to 350°C at vapor saturation pressures. Am. J. Sci. 299, 173–209.] and that of Shock and Helgeson [Shock, E.L., Helgeson, H.C., 1988. Calculation of the thermodynamic and transport properties of aqueous species at high pressures and temperatures: correlation algorithms for ionic species and equation-of-state predictions to 5 kb and 1000°C. Geochim. Cosmochim. Acta 53, 2009–2036.] and Shock et al. [Shock, E.L., Oelkers, E.H., Johnson, J.W., Sverjensky, D.A., Helgeson, H.C., 1992. Calculation of the thermodynamic properties of aqueous species at high pressures and temperatures: effective electrostatic radii, dissociation constants, and standard partial molal properties to 1000°C and 5 kbar. J. Chem. Soc., Faraday Trans. 88, 803–826.] for most aqueous species. For aqueous $Fe(OH)_4^-$ and $Al(OH)_4^-$, the thermodynamic properties reported by Diakonov et al. and Pokrovskii and Helgeson [Pokrovskii, V.A., Helgeson, H.C., 1995. Thermodynamic properties of aqueous species and the solubilities of minerals at high pressures and temperatures: the system Al_2O_3–H_2O–NaCl. Am. J. Sci. 295, 1255–1342], respectively, were used. In the present study, the standard partial molal properties and the HKF equation-of-state parameters for aqueous $H_4SiO_4^0$ were revised to better describe the recent experimental results at low temperatures. For $H_4SiO_4^0$, the new parameters are also consistent with quartz solubility experiments up to 900°C and 5 kbar. Further, the HKF equation-of-state parameters for aqueous $Ti(OH)_4^0$ were estimated from rutile solubility [Ziemniak, S.E., Jones, M.E., Combs, K.E.S., 1993. Solubility behaviour of titanium (IV) oxide in alkaline media at elevated temperatures. J. Sol. Chem. 22, 601–623.], which enables the calculations of the solubility of Ti-bearing minerals at elevated temperatures and pressures. Much higher solubilities were found for the silicate minerals below 100°C than previously reported, which is related to higher quartz solubility at low temperature and correspondingly new data on the thermodynamic properties of $H_4SiO_4^0$. The present results

* Institut fur Mineralogie und Petrographie (IMP), ETH-Zentrum, Sonneggstrasse 5, 8092 Zurich, Switzerland. Tel.: +41-1-632-7803; fax: +41-1-632-1088.

E-mail address: andri@erdw.ethz.ch (A. Stefánsson).

PII: S0009-2541(00)00263-1

are particularly important for the stabilities of primary basaltic minerals of natural composition under weathering conditions. They are also of importance for the study of equilibrium/dis-equilibrium conditions in active geothermal systems.

Keywords: Basalt; Solubility; Mineral solid solutions; Aqueous silica; Aqueous titanium

1. Introduction

The major input of chemical constituents into natural aqueous systems comes from mineral dissolution. Knowledge of mineral solubilities and their mode and rate of dissolution is essential for interpretation of water–rock interaction and the transport of dissolved solids in river and ground water systems.

The primary minerals of basaltic rocks, which include olivine, plagioclase, pyroxene, Fe–Ti oxide and sometimes apatite, all form solid solutions between two or more end-members. In order to predict the saturation state of natural waters with respect to these minerals, one needs to be able to evaluate the thermodynamic properties of their solid solutions as well as of the aqueous species they form upon dissolution.

The thermodynamics of mixing and exchange of atoms in minerals has received considerable attention in recent years (e.g., Saxena and Ghose, 1971; Saxena et al., 1974; McCallister et al., 1976; Newton et al., 1980; Sack, 1980, 1982; Sack and Ghiorso, 1989, 1991, 1994a,b; Wood and Kleppa, 1981; O'Neill and Navrotsky, 1984; Carpenter et al., 1985; Davidson and Lindsley, 1985; Anderson and Lindsley, 1988; Hackler and Wood, 1989; Ghiorso, 1990; Wiser and Wood, 1991; von Seckendorff and O'Neill, 1993; Kojitani and Akaogi, 1994; Berman and Aranovich, 1996; Berman et al., 1995) and the relationship between mineral solid solutions and aqueous solutions (Helgeson and Aagaard, 1985; Glynn and Reardon, 1990). Most of these studies focused on systems at elevated temperatures (600–1400°C), which is far from the temperature regime of most accessible natural waters (0–350°C).

When studying the saturation state of natural waters in Iceland with respect to olivine, orthopyroxene, and plagioclase, Gíslason and Arnórsson (1990, 1993) expressed the standard state as that of an ideal solid solution of fixed composition. Gíslason et al. (1996a,b) and Brady and Gíslason (1997) used the same thermodynamic approach when calculating the saturation state of global average river water with respect to these minerals as a function of pH, and the saturation state of these minerals in seawater as a function of temperature.

The aim of the present study is to derive the solubility constants of primary minerals of basalt in pure water in the temperature range 0–350°C at saturated water vapour pressure. Such conditions effectively cover the *P–T* environment of natural waters, and enables one to deduce by comparison between these solubility constants and reaction quotients (activity products) whether a particular water is at equilibrium under or supersaturated with respect to these minerals. The state of saturation of these minerals in a range of natural waters associated with basaltic rocks is the subject of another contribution (Stefánsson et al., 2000).

2. Dissolution reactions of primary minerals of basalt

The dissolution reactions for primary minerals of basalt in aqueous solution used in the present study are given in Table 1. They have been expressed in terms of those aqueous species that were generally found to be dominant in natural waters in the basaltic terrain of Iceland (see Stefánsson et al., 2000). By expressing the reactions in terms of the dominant aqueous species, errors in calculated reaction quotients (activity products) were minimized, at least in those cases where the selected aqueous species were the dominant ones. In general, the accuracy by which activity product is calculated depends on the quality of the analytical data, the thermodynamic database and how accurate the reference temperature is at which chemical speciation is calculated.

Table 1
Dissolution reactions of primary minerals of basalt

Mineral	Composition[a]	Reaction
Olivine	Fo_{100}	$Mg_2SiO_4 + H^+ = 2Mg^{2+} + H_4SiO_4^0$
	Fa_{100}	$Fe_2SiO_4 + H^+ = 2Fe^{2+} + H_4SiO_4^0$
	$Fo_{80}Fa_{20}$	$(Mg_{0.80}Fe_{0.20})_2SiO_4 + H^+ = 1.60Mg^{2+} + 0.40Fe^{2+} + H_4SiO_4^0$
	$Fo_{43}Fa_{53}$	$(Mg_{0.43}Fe_{0.57})_2SiO_4 + H^+ = 0.86Mg^{2+} + 1.14Fe^{2+} + H_4SiO_4^0$
Pyroxene	En_{100}	$MgSiO_3 + 2H^+ + H_2O = Mg^{2+} + H_4SiO_4^0$
	Fs_{100}	$FeSiO_3 + 2H^+ + H_2O = Fe^{2+} + H_4SiO_4^0$
	Di_{100}	$Mg_{0.5}Ca_{0.5}SiO_3 + 2H^+ + H_2O = 0.5Ca^{2+} + 0.5Mg^{2+} + H_4SiO_4^0$
	Hed_{100}	$Fe_{0.5}Ca_{0.5}SiO_3 + 2H^+ + H_2O = 0.5Ca^{2+} + 0.5Fe^{2+} + H_4SiO_4^0$
	$En_{38}Fs_{62}$	$Mg_{0.38}Fe_{0.62}SiO_3 + 2H^+ + H_2O = 0.38Mg^{2+} + 0.62Fe^{2+} + H_4SiO_4^0$
	$Di_{45}Hed_{25}En_{19}Fs_{11}$	$Ca_{0.35}Mg_{0.42}Fe_{0.23}SiO_3 + 2H^+ + H_2O = 0.35Ca^{2+} + 0.42Mg^{2+} + 0.23Fe^{2+} + H_4SiO_4^0$
Plagioclase	An_{100}	$CaAl_2Si_2O_8 + 8H_2O = Ca^{2+} + 2Al(OH)_4^- + 2H_4SiO_4^0$
	Ab_{100}	$NaAlSi_3O_8 + 8H_2O = Na^+ + Al(OH)_4^- + 3H_4SiO_4^0$
	$An_{70}Ab_{30}$	$Ca_{0.70}Na_{0.30}Al_{1.70}Si_{2.30}O_8 + 8H_2O = 0.70Ca^{2+} + 0.30Na^+ + 1.70Al(OH)_4^- + 2.30H_4SiO_4^0$
	$An_{29}Ab_{71}$	$Ca_{0.29}Na_{0.71}Al_{1.29}Si_{2.71}O_8 + 8H_2O = 0.29Ca^{2+} + 0.71Na^+ + 1.29Al(OH)_4^- + 2.71H_4SiO_4^0$
Magnetite–ulvöspinel	Mt_{100}	$FeFe_2O_4 + 4H_2O = Fe^{2+} + 2Fe(OH)_4^-$
	Usp_{100}	$Fe_2TiO_4 + 4H^+ = 2Fe^{2+} + Ti(OH)_4^0$
	$Mt_{15}Usp_{85}$	$Fe^{2+}_{1.85}Fe^{3+}_{0.3}Ti_{0.85}O_4 + 3.4H^+ + 0.6H_2O = 1.85Fe^{2+} + 0.30Fe(OH)_4^- + 0.85Ti(OH)_4^0$
	$Mt_{68}Usp_{32}$	$Fe^{2+}_{1.32}Fe^{3+}_{1.36}Ti_{0.32}O_4 + 1.28H^+ + 2.72H_2O = 1.32Fe^{2+} + 1.36Fe(OH)_4^- + 0.32Ti(OH)_4^0$
Hematite–ilmenite	Hem_{100}	$Fe_2O_3 + 5H_2O = 2Fe(OH)_4^- + 2H^+$
	Ilm_{100}	$FeTiO_3 + H_2O + 2H^+ = Fe2^+ + Ti(OH)_4^0$
	Hem_7Ilm_{93}	$Fe^{2+}_{0.93}Fe^{3+}_{0.14}Ti_{0.93}O_4 + 172H^+ + 1.28H_2O = 0.93Fe^{2+} + 0.14Fe(OH)_4^- + 0.93Ti(OH)_4^0$
Apatite	F-Ap_{100}	$Ca_5(PO_4)_3F + 3H^+ = 5Ca^{2+} + 3HPO_4^{2-} + F^-$
	OH-Ap_{100}	$Ca_5(PO_4)_3OH + 3H^+ = 5Ca^{2+} + 3HPO_4^{2-} + OH^-$

[a] The mineral solid solutions represent average groundmass composition of the respective mineral in Icelandic volcanics as calculated by Gíslason and Arnórsson (1990, 1993) using data from Carmichael (1967) and Fisk (1978). For Ca-rich clinopyroxene and orthopyroxene, average composition have been calculated from compositinal range given by Gíslason and Arnórsson (1990).

The deduction of the generally predominant aqueous species in natural waters associated with basaltic rocks in Iceland were made from the database on water compositions given in Stefánsson et al. (2000). The WATCH program (Arnórsson et al., 1982) version 2.1A (Bjarnason, 1994) was used for the aqueous speciation calculations. The thermodynamic database in the WATCH program is that of Arnórsson et al. (1982, Table 5) except for Al-hydroxy complexes and gas solubilities (Arnórsson and Andrésdóttir, 1999; Arnórsson et al., 2000). For the present study, the thermodynamic properties of Fe^{III}-hydroxy complexes of the WATCH program were revised according to data given by Diakonov et al. (1999) and Diakonov and Tagirov (2000). Also, a supplement was added to the program to include phosphoro-oxy anions (Shock and Helgeson, 1988; Shock et al., 1997), Fe, Mg and Ca phosphates (Kharaka and Barnes, 1973) and Ti-hydroxy and Ti-phosphate species (Ziemniak et al., 1993). For further details of the speciation calculations and distribution of aqueous species in natural waters in Iceland, the reader is referred to Stefánsson et al. (2000).

3. Thermodynamic relations

Changes in the apparent standard partial molal Gibbs energy with temperature and pressure are given by

$$\Delta\overline{G}^0_{T,P,i} = \Delta G^0_{f,T_r,P_r,i} - S^0_{T_r,i}(T - T_r) + \int_{T_r}^{T} C^0_{p,i}\,dT - T\int_{T_r}^{T} C^0_{p,i}/T\,dT + \int_{P_r}^{P} V^0_{T,i}\,dP \quad (1)$$

Table 2
Thermodynamic properties for aqueous species[a]

Species	$\Delta G^0_{f,T_r}$ (J mol^{-1})	$\Delta H^0_{f,T_r}$ (J mol^{-1})	$S^0_{T_r}$ (J mol^{-1} K^{-1})	$C^0_{P_r}$ (J mol^{-1} K^{-1})	$V^0_{T_r}$ (cm^3 mol^{-1})	$a_1 \times 10$ (J mol^{-1} bar^{-1})	$a_2 \times 10^{-2}$ (J mol^{-1})	a_3 (J K mol^{-1} bar^{-1})	$a_4 \times 10^{-4}$ (J K mol^{-1})	c_1 (J mol^{-1} K^{-1})	$c_2 \times 10^{-4}$ (J K mol^{-1})	$\omega \times 10^{-5}$ (J mol^{-1})
Na^+	−261,881	−240,300	58.4	37.9	−1.11	7.694	−9.560	13.623	−11.406	76.07	−12.473	1.3832
K^+	−282,462	−252,170	101.0	8.3	9.06	14.891	−6.163	22.740	−11.347	30.96	−7.494	0.8063
Ca^{2+}	−552,790	−543,083	−56.5	−31.5	−18.06	−0.815	−30.342	22.161	−10.373	37.66	−10.552	5.1739
Mg^{2+}	−453,985	−465,960	−138.1	−22.3	−21.55	−3.438	−35.978	35.104	−10.000	87.03	−24.652	6.4316
Fe^{2+} [b]	−91,504	−92,257	−105.9	−33.1	−22.2	−3.292	−40.572	39.948	−9.950	61.86	−19.429	6.0174
OH^-	−157,297	−230,024	−10.7	−137.2	−4.18	5.241	0.309	7.708	−11.640	17.36	−43.288	7.2157
F^-	−281,751	−335,348	−13.2	−113.9	−1.32	2.874	5.685	31.812	−11.862	18.66	−31.330	7.4768
HPO_4^{2-}	−1,089,137	−1,292,082	−33.5	−243.9	5.4	15.194	4.543	22.273	−11.815	11.45	−62.385	13.9591
$Fe(OH)_4^-$ [c]	−845,026	−1,050,791	74.1	105.7	56.86	41.542	68.921	−3.036	−14.477	375.68	−113.729	4.2614
AlO_2^- [d]	−831,361	−929,179	−29.3	−39.7	9.5	15.598	16.652	−6.3471	−12.316	79.91	−25.941	7.3617

[a] Unless otherwise indicated, the data are from Shock and Helgeson (1988).
[b] Shock et al. (1997).
[c] Diakonov et al. (1999).
[d] Pokrovskii and Helgeson (1995).

Table 3
Thermodynamic properties for aqueous species extracted in the present study

Species	$\Delta G^0_{f,T_r}$ (J mol^{-1})	$\Delta H^0_{f,T_r}$ (J mol^{-1})	$S^0_{T_r}$ (J mol^{-1} K^{-1})	$C^0_{P_r}$ (J mol^{-1} K^{-1})	$V^0_{T_r}$ (cm^3 mol^{-1})	$a_1 \times 10$ (J mol^{-1} bar^{-1})	$a_2 \times 10^{-2}$ (J mol^{-1})	a_3 (J K mol^{-1} bar^{-1})	$a_4 \times 10^{-4}$ (J K mol^{-1})	c_1 (J mol^{-1} K^{-1})	$c_2 \times 10^{-4}$ (J K mol^{-1})	$\omega \times 10^{-5}$ (J mol^{-1})
$Ti(OH)^0_4$	−1,312,480[a]	−1,511,809[b]	21.92	202.9	40.6[c]	30.823[d]	42.719[d]	4.824[d]	−13.393[d]	214.54	−5.341	0.0627
$H4SiO^0_4$	−1,309,257	−1,458,861[b]	188.70	62.8	52.3	78.366	−88.952	77.906	−5.021	242.80	−86.985	0.3636

[a] Ziemniak et al. (1993).
[b] Calculated from the ΔG^0_f and S^0 values in the table together with the S^0 of the element given by Cox et al. (1989).
[c] Calculated from empirical correlation between S^0 and V^0 given by Shock et al. (1997, Table 9).
[d] Estimated from correlations given by Shock and Helgeson (1988).

Table 4
Thermodynamic properties of primary basaltic minerals at 25°C and 1 bar[a]

Mineral	Formula	$\Delta G^0_{f,T_r}$ (kJ mol^{-1})	$\Delta H^0_{f,T_r}$ (mJ mol^{-1})	$S^0_{T_r}$ (J mol^{-1} K^{-1})	$V^0_{T_r}$ (cm^3 mol^{-1})	$C^0_{P_r} = a + bT + cT^{-2} + fT^2 + gT^{-0.5}$				
						$a\times10^{-2}$ (J mol^{-1})	$b\times10^{2}$ (J mol^{-1} K^{-2})	$c\times10^{-6}$ (J K mol^{-1})	$f\times10^{5}$ (J mol^{-1} K^{-3})	g$\times10^{-3}$ (J mol^{-1} K$^{-0.5}$)
Fayalite	Mg_2SiO_2	−1379.1	−1478.2	151.0	46.310	1.7602	−0.8808	−3.889	2.471	
Forsterite	Fe_2SiO_4	−2053.6	−2173.0	94.1	43.650	0.8736	8.717	−3.699	−2.237	0.8436
Hedenbergite	$CaFeSi_2O_6$	−2676.3	−2839.9	174.2	67.950	3.1046	1.257	−1.846		−2.040
Diopside	$CaMgSi_2O_6$	−3026.8	−3201.5	142.7	66.090	4.7025	−9.864	0.2454	2.813	−4.823
Ferrosilite	$FeSiO_3$	−1118.0	−1195.2	94.6	33.000	1.243	1.454	−3.378		
Enstatite	$MgSiO_3$	−1458.3	−1545.6	66.3	31.310	3.507	−14.72	1.769	5.826	−4.296
Clinoenstatite	$MgSiO_3$	−1458.1	−1545.0	67.9	31.280	2.056	−1.280	1.193		−2.298
Anorthite	$CaAl_2Si_2O_8$	−4002.1[b]	−4227.8[b]	199.3[b]	100.79[b]	5.168	−9.249	−1.408	4.188	−4.589
Albite (high)	$NaAlSi_3O_8$	−3705.1[b]	−3923.4[b]	224.4[b]	100.83[b]	6.714	−14.67	3.174	3.659	−7.974
“C1 anorthite”	$CaAl_2Si_2O_8$	−3990.3[b]	−4213.8[b]	206.6[b]	100.79[b]	5.168	−9.249	−1.408	4.188	−4.589
“High I1 albite”	$NaAlSi_3O_8$	−3669.8[b]	−3888.1[b]	224.4[b]	100.83[b]	6.714	−14.67	3.174	3.659	−7.974
Ilmenite	$FeTiO_3$	−1155.5	−1232.0	108.9	31.690	2.627	−7.999	0.3827	3.388	−2.538
Ulvospinel	Fe_2TiO_4	−1399.9	−1493.8	180.4	46.820	−1.026	14.25	−9.145		5.271
Hematite	Fe_2O_3	−744.4	−826.2	87.4	30.270	15.0147	−121.46	14.123	56.90	−21.493
Magnetite	Fe_3O_4	−1012.7	−1115.7	146.1	44.520	26.5911	−252.15	20.734	136.77	−36.455
Fluorapatite	$Ca_5(PO_4)_3F$	−6489.7	−6872.0	387.9	157.560	7.543	−3.026	−0.9084		−6.201
Hydroxyapatite	$Ca_5(PO_4)_3OH$	−6337.1	−6738.5	390.4	159.600	3.878	11.860	−12.70		1.811

[a]Unless otherwise indicated, the data are from Robie and Hemingway (1995).
[b]Arnórsson and Stefánsson (1999).

where $\Delta\overline{G}_i^0$ stands for the apparent standard partial molal Gibbs energy of the *i*-th mineral or aqueous species, i.e. the standard state of Helgeson et al. (1981) was used. The same relationship holds, of course, for the standard molal Gibbs energy of reaction.

In the present study the integral in Eq. (1) for aqueous species was solved with the aid of the revised HKF equation-of-state (Helgeson et al., 1981; Tanger and Helgeson, 1988; Shock and Helgeson, 1988; Shock et al., 1992) using the HKF equation-of-state parameters given in Tables 2 and 3.

For the basaltic primary minerals, the heat capacities at 1 bar between 0°C and 350°C was calculated using the heat capacity polynomial

$$C_{p,i}^0 = a + bT + cT^{-2} + fT^2 + gT^{-0.5} \quad (2)$$

where *a*, *b*, *c*, *f* and *g* are the temperature-independent heat capacity parameters given in Tables 4 and 6.

It was considered convenient to describe the temperature dependence of the standard Gibbs energy of dissolution reactions of primary basaltic minerals at saturated water vapour pressure, as these conditions are close to those in most natural aqueous systems. Under these pressure conditions, the molal volume of minerals (V^0) is almost constant, i.e. the pressure dependence of $\Delta\overline{G}^0$ for minerals was taken to be

$$\int_{P_r}^{P} V_{T,i}^0 = V_{T_r,i}^0 (P - P_r) \quad (3)$$

The Gibbs energy of reaction is defined as

$$\Delta G_{T,P,r}^0 = \sum_i \nu_i \Delta\overline{G}_{T,P,i}^0 \quad (4)$$

where ν_i denotes the stoichiometric coefficient of the *i*-th aqueous species or mineral in the reaction, which is positive for products and negative for reactants.

The equilibrium constant is related to the standard Gibbs energy of a reaction at any temperature and pressure by

$$\log K = \frac{\Delta G_{T,P,r}^0}{-RT\ln(10)} \quad (5)$$

where *R* and *T* are the gas constant and temperature in Kelvin, respectively.

4. Thermodynamic properties of aqueous species

In most cases, the thermodynamic properties of aqueous species were selected from Shock and Helgeson (1988) and Shock et al. (1997), i.e. the SUPCRT92 database was used, including calculations of $\Delta\overline{G}^0$ for H_2O (Johnson et al., 1992). However, for aqueous $H_4SiO_4^0$ and $Ti(OH)_4^0$ the thermodynamic properties and the HKF equation-of-state parameters were revised and retrieved, respectively, for the present study according to recent experimental results. Also, the thermodynamic properties for $Fe(OH)_4^-$ and $Al(OH)_4^-$ were selected from Diakonov et al. (1998a) and Pokrovskii and Helgeson (1995), respectively. The thermodynamic properties, especially of those aqueous species not selected from Shock and Helgeson (1988) and Shock et al. (1997) (SUPCRT92), are discussed below.

4.1. Na^+, K^+, Ca^{2+}, Mg^{2+}, Fe^{2+} and HPO_4^{2-}

The thermodynamic properties of Na^+, K^+, Ca^{2+} and Mg^{2+} at 25°C and 1 bar are accurately known and those for Fe^{2+} and HPC_4^{2-}, reasonably accurately. For the first four ions and HPO_4^{2-}, the values reported by Shock and Helgeson (1988) were selected but for Fe^{2+}, the values given by Shock et al. (1997) were used. The apparent standard partial molal Gibbs energy for all these species at elevated temperatures at saturated water vapour pressure were obtained from the equation-of-state parameters in the HKF model of Helgeson et al. (1981), Tanger and Helgeson (1988), Shock and Helgeson (1988), and Shock et al. (1992) using the HKF equation-of-state parameters given in Shock and Helgeson (1988) and Shock et al. (1997).

4.2. $Fe(OH)_4^-$

The thermodynamic properties of aqueous $Fe(OH)_4^-$ have been extracted from room temperature solubility measurements of amorphous iron hy-

droxides (Biederman and Schindler, 1957; Lengweiler et al., 1961a,b; Byrne and Kester, 1976; Kuma et al., 1993), goethite solubility (Kamnev et al., 1986), hematite solubility experiments at high temperatures (Sergeyeva et al., 1988; Dillenseger, 1995; Ziemniak et al., 1995; Diakonov et al., 1999) and empirical correlations (Shock et al., 1997).

Some discrepancies exist between measured hematite solubility at 200–300°C. Diakonov et al. (1999) argued that the higher solubility of hematite measured by Dillenseger (1995) and Sergeyeva et al. (1988) could be explained by the formation of a Na/K–Fe complex and demonstrated that if their experimental results were corrected for Na/K–Fe complexes with a stability equal to $NaAl(OH)_4^0$ (Diakonov et al., 1996), all hematite solubility experiments were in good agreement and showed a linear correlation between log K and $1/T$ below 250°C.

Based on hematite solubility, Diakonov et al. (1999) calculated the standard Gibbs energy of formation from the elements (ΔG_f^0) for $Fe(OH)_4^-$ as $-845{,}042$ J mol^{-1} at 25°C and 1 bar. This value is more negative than that reported by Shock et al. (1997) of $-842{,}557$ J mol^{-1}, which was retrieved from hydrolysis constants given by Baes and Mesmer (1976, 1981) and ΔG_f^0 of $Fe(OH)_4^-$ at 25°C and 1 bar as $-842{,}239$ J mol^{-1} and $-840{,}218$ J mol^{-1}, respectively, based on magnetite solubility at elevated temperatures.

Kamnev et al. (1986) measured the solubility of goethite in alkaline solution at 20°C. Diakonov et al. (1994) showed that in alkaline solution goethite surface area decreases with time, which in turns affects its solubility. Correcting the experimental results of Kamnev et al. (1986) for initial and final goethite surfaces (Diakonov et al., 1994) and water (SUPCRT92), the Gibbs energy of formation for $Fe(OH)_4^-$ 20°C is -844.6 kJ mol^{-1}. Thus, the results of Kamnev et al. (1986) and Diakonov et al. (1999) are in excellent agreement, supporting the validity of Diakonov et al.'s (1999) results on the thermodynamic properties of $Fe(OH)_4^-$, which were selected for the present study.

The $\Delta\overline{G}^0$ of $Fe(OH)_4^-$ from 0°C to 350°C derived from Diakonov et al. (1999) and Shock et al. (1997) are compared in Fig. 1. Also shown in the figure are values derived from experimental work on hematite and goethite solubilities. Considerable difference exists in the values predicted by Diakonov et al. (1999) and Shock et al. (1997). However, as clearly indicated, the values suggested by Diakonov et al. (1999) correlate better with hematite solubility than the values of Shock et al. (1997).

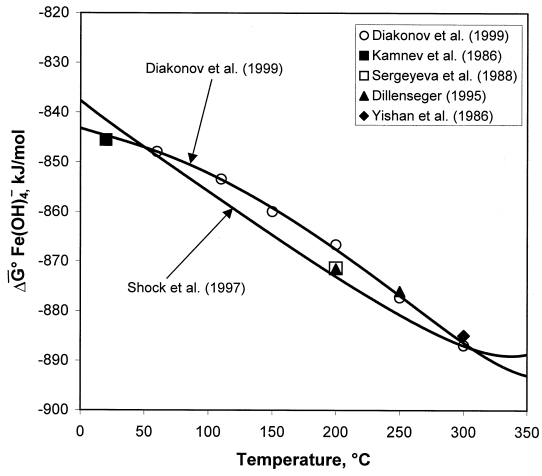

Fig. 1. Comparision of the apparent standard Gibbs energy for $Fe(OH)_4^-$ 350°C and saturated water vapour pressures. The curves show the calculated values obtained using the thermodynamic properties and HKF equation-of-state parameters reported by Shock et al. (1997) and Diakonov et al. (1999). The symbols represent values derived from experiments of goethite and hematite solubility as given in Diakonov et al. (1999), Yishan et al., 1986.

4.3. $Al(OH)_4^-$

The thermodynamic properties of the $Al(OH)_4^-$ have mostly been extracted from gibbsite and boehmite solubility experiments in alkaline solutions. Verdes et al. (1992) summarized experimental work on gibbsite solubility while Castet et al. (1993) summarized those on boehmite solubility and Pokrovskii and Helgeson (1995) on both minerals.

There is generally good conformity for the Gibbs energy of formation from the elements for $Al(OH)_4^-$ 25°C (Apps et al., 1989; Verdes et al., 1992; Wesolowski, 1992; Castet et al., 1993; Pokrovskii and Helgeson, 1995; Diakonov et al., 1996; Shock et al., 1997; Arnórsson and Andrésdóttir, 1999). By contrast, there are some differences at elevated temperatures particularly above 300°C (Fig. 2).

Diakonov et al. (1996) estimated the HKF equation-of-state parameters for $Al(OH)_4^-$ from the ex-

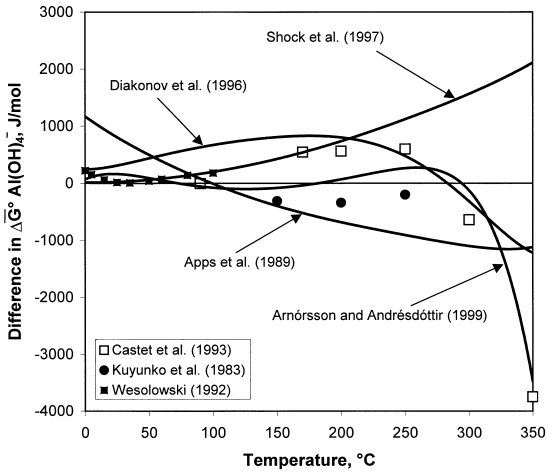

Fig. 2. Difference in the apparent standard Gibbs energy for $Al(OH)_4^-$ 350°C and saturated water vapour pressure between that of Pokrovskii and Helgeson (1995) and various other researches as indicated. The symbols represent experimental values based on gibbsite, boehmite and diaspore solubilities and the thermodynamic data of the minerals and water as given by Robie and Hemingway (1995) and in SUPCRT92 (Johnson et al., 1992), Kuyunko et al., 1983.

perimental results of Castet et al. (1993). However, at low temperatures, their $\Delta\overline{G}^0$ values are systematically lower (more negative) than the corresponding values obtained from experimental results of gibbsite solubility (Wesolowski, 1992). Shock et al. (1997) calculated the thermodynamic properties of the aluminate ion AlO_2^- from gibbsite solubility below 100°C (Wesolowski, 1992). In order to avoid uncertainties at higher temperatures and inconsistency concerning the gibbsite solubility in acidic solutions, Shock et al. (1997) employed the data of Couturier et al. (1984) for the reaction $Al^{3+} + 2H_2O = AlO_2^- + 4H^+$. As clearly indicated in Fig. 2, the calculated $\Delta\overline{G}^0$ values using the data of Shock et al. (1997) are in excellent agreements with experimental results of boehmite and gibbsite solubility (Wesolowski, 1992; Castet et al., 1993) at temperatures below 200°C. At higher temperatures their values deviate considerably; by about 2000 J mol^{-1} at 300°C.

Pokrovskii and Helgeson (1995) extracted the thermodynamic properties of aqueous species in the system Al_2O_3–H_2O–NaCl from solubility experiments of gibbsite, boehmite and diaspore given in the literature (see Pokrovskii and Helgeson, 1995, for reference). Pokrovskii and Helgeson (1995) argued that a considerable proportion of total aqueous Al in sodium-bearing alkaline solutions is present as $NaAl(OH)_4^0$ and reinterpreted previous experimental results taking this complex into account. As seen in Fig. 2, the $\Delta\overline{G}^0$ values calculated using the thermodynamic properties of $Al(OH)_4^-$ HKF equation-of-state parameters reported by Pokrovskii and Helgeson (1995) compare reasonably well with experimentally derived values.

Arnórsson and Andrésdóttir (1999) reviewed the thermodynamic properties of aqueous Al-hydroxy complexes in the temperature range 0–350°C at saturated water vapour pressure. They selected the proposed values of ΔH_r, ΔS_r and ΔG_r of gibbsite solubility in alkaline solution at 25°C of Wesolowski (1992) and combined this with the thermodynamic properties of gibbsite and water (Hemingway and Robie, 1977; Hemingway et al., 1977; Cox et al., 1989) to obtain $\Delta G_f^0 = 1{,}305{,}575$ J mol^{-1}, $\Delta H_f^0 = -1{,}500{,}640$ J mol^{-1} and $S^0 = 111.1$ J mol^{-1} K^{-1} for $Al(OH)_4^-$ at 25°C and 1 bar. At higher temperatures and pressures, the $\Delta\overline{G}^0$ values for $Al(OH)_4^-$ from their reported thermodynamic properties are consistent with boehmite solubility given in the literature (see Arnórsson and Andrésdóttir, 1999, for reference).

In the present study, the thermodynamic properties of $Al(OH)_4^-(AlO_2^- + 2H_2O)$ and the HKF equation-of-state parameters given by Pokrovskii and Helgeson (1995) were selected. The results of Pokrovskii and Helgeson (1995) are close to the average of the calculated $\Delta\overline{G}^0$ according to the values given in Fig. 2, and are consistent with a number of experimental results and are very close to the values selected by Arnórsson and Andrésdóttir (1999) up to 300°C. The WATCH speciation program (Arnórsson et al., 1982) uses the thermodynamic database of Al-hydroxy complexes given in Arnórsson and Andrésdóttir (1999). The thermodynamic properties of $Al(OH)_4^-$ selected in the present study are, therefore, considered to be consistent with that used in the speciation calculations (Stefánsson et al., 2000).

4.4. $H_4SiO_4^0$

On the basis of their experimental results of amorphous silica solubility and experimental data of

amorphous silica and quartz solubility given in the literature, Gunnarsson and Arnórsson (2000) calculated the thermodynamic properties of $H_4SiO_4^0$ in the range 0–350°C. Their results below 100°C are in excellent agreement with those of Rimstidt (1997) obtained from quartz solubility experiments in the temperature range 21–96°C. Also, Gunnarsson and Arnórsson (2000) observed that the thermodynamic data for amorphous silica and its solubility yielded $\Delta\overline{G}^0$ values for $H_4SiO_4^0$ very similar to those derived from quartz solubility data (within ± 500 J mol^{-1}).

The value of the Gibbs energy of formation from the elements for $H_4SiO_4^0$ reported by Rimstidt (1997) and Gunnarsson and Arnórsson (2000) are more negative than generally accepted (e.g., Shock et al., 1989) or by 1500 J mol^{-1} at 25°C and by 3000 J mol^{-1} at 0°C. Gunnarsson and Arnórsson (2000) argued that the reason for the much lower quartz solubility measured by Fournier (1960), Morey et al. (1962) and Mackenzie and Gees (1971) below 100°C compared to that measured by Rimstidt (1997) and van Lier et al. (1960) is likely to be due to a failure to attain equilibrium because of slow reaction rates. They further argued that the good agreement between the Gibbs energy of $H_4SiO_4^0$ in the range 0–350°C as calculated from amorphous silica solubility data, on one hand, and quartz solubility on the other support the validity of the quartz solubility results of Rimstidt (1997).

In the present study, the standard partial molal thermodynamic properties and the HKF equation-of-state parameters for $H_4SiO_4^0$ were revised to better describe quartz and amorphous silica solubilities at low temperature as measured by Rimstidt (1997) and Gunnarsson and Arnórsson (2000). These data were obtained by first calculating the quartz solubility in the temperature range 0–350°C using the data of Gunnarsson and Arnórsson (2000), which was, in turn, based on data given by Kennedy (1950), Fournier (1960), Kitahara (1960), Van Lier et al. (1960), Morey et al. (1962), Siever (1962), Crerar and Anderson (1971), Mackenzie and Gees (1971), Hemley et al. (1980) and Rimstidt (1997). At higher temperatures and pressures (up to 900°C and 5 kbar), the quartz solubility data of Kennedy (1950), Morey and Hesselgesser (1951), Khitarov (1956), Weill and Fyfe (1964), Anderson and Burnham (1965, 1967) and Hemley et al. (1980) were used. These solubilities were then combined with the thermodynamic properties of quartz (Helgeson et al., 1978) and water (SUPCRT92) to calculate the standard apparent Gibbs energy of $H_4SiO_4^0$ at a given temperature and pressure. Subsequently, these $\Delta\overline{G}^0$ were fitted using a linear least square method to generate the HKF equation-of-state parameters (c_1, c_2, a_1, a_2, a_3, a_4), the effective Born coefficient (ω), and the ΔG_f^0, S^0, V^0 and C_p^0 values at 25°C and 1 bar. The results are given in Table 3.

The value for the standard Gibbs energy of formation from the elements at 25°C for $H_4SiO_4^0$ obtained in the present study is $-1{,}309{,}257$ J mol^{-1} and in excellent agreement with those reported by Gunnarsson and Arnórsson (2000) ($-1{,}309{,}181$ J mol^{-1}) and Rimstidt (1997) ($-1{,}309{,}231$ J mol^{-1}). However, the value of Shock et al. (1989) is more than 2000 J mol^{-1} less negative. Also, the standard partial entropy of 188.70 J mol^{-1} K^{-1} obtained in the present study closely matches recent estimation given by Nordstom and Munoz (1994), Rimstidt (1997) and Gunnarsson and Arnórsson (2000) of 189.5, 180.87 and 178.85 J mol^{-1} K^{-1}, respectively. The value given by Shock et al. (1989) of 215.16 J mol^{-1} K^{-1} ($S^0_{SiO_{4(aq)}} + 2S_{H_2O}{}^0$) does not, however, correspond well to the other entropy values.

The differences in $\Delta\overline{G}^0$ for $H_4SiO_4^0$ as derived in the present study and those of Shock et al. (1989), Rimstidt (1997) and Gunnarsson and Arnórsson (2000) are compared in Fig. 3. There is good agreement between the values derived in the present study based and those of Gunnarsson and Arnórsson (2000) and Rimstidt (1997). However, considerable discrepancies exist between the values selected here and those reported by Shock et al. (1989) especially at low temperatures (< 50°C).

Quartz solubility calculated from the thermodynamic properties on aqueous silica obtained in the present study and the thermodynamic properties of quartz (Helgeson et al., 1978) and water (SUPCRT92) are compared with experimental values at elevated temperatures and pressures in Fig. 4. As clearly seen from Fig. 4, the values (curves) obtained in the present study agree well with the experimental results at all temperatures and pressures.

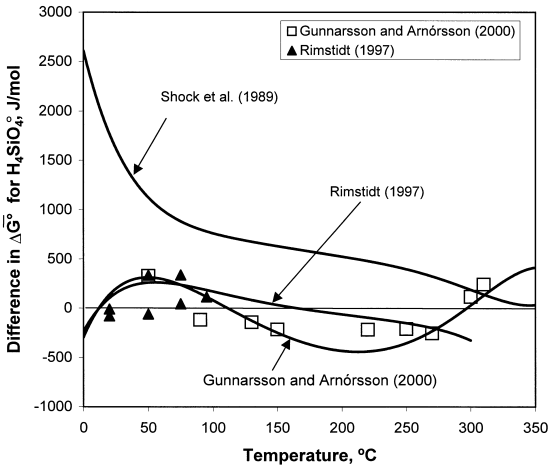

Fig. 3. The difference in calculated apparent standard Gibbs energy for $H_4SiO_4^0$ of this study and those given by Shock et al. (1989), Rimstidt (1997) and Gunnarsson and Arnórsson (2000). Also shown are the values derived from experiments of amorphous silica and quartz as indicated.

4.5. $Ti(OH)_4^0$

Some experiments have been carried out to determine the solubility of hydrous TiO_2 precipitated from solution and equilibrated for various lengths of time (e.g., Babko et al., 1962; Liberti et al., 1963). Despite differences in experimental conditions such as temperature, medium and particle size, the results are in good agreement. On the basis of these experimental results and by assuming that rutile was about four orders of magnitude less soluble than hydrous TiO_2, Baes and Mesmer (1976) estimated the solubility of rutile and the hydrolysis constants between $Ti(OH)_2^{2+}$, $Ti(OH)_3^+$ and $Ti(OH)_4^0$. From these results and the standard Gibbs energy of formation from the elements of rutile at 25°C of -889.5 kJ mol^{-1} (Robie and Hemingway, 1995) and water (SUPCRT92), $Ti(OH)_2^{2+}$, $Ti(OH)_3^+$ and $Ti(OH)_4^0$ of -862.1, -1086.7 and -1309.0 kJ mol^{-1} are obtained, respectively.

Ziemniak et al. (1993) measured the solubility of rutile in aqueous sodium phosphate, sodium hydroxide and ammonium hydroxide solutions between 17°C and 288°C. They further summarized the thermodynamic properties of aqueous species in the system TiO_2–H_2O and TiO_2–P_2O_5–H_2O. From their experimental results, Ziemniak et al. (1993) obtained a ΔG_f^0 value at 25°C for $Ti(OH)_4^0$ and $Ti(OH)_5^-$ of -1312.46 and -1479.20 kJ mol^{-1}, respectively. The former value is well within the uncertainty of estimation of Baes and Mesmer (1976). Further, assuming isocolombic conditions for rutile dissolution and the fifth Ti-hydrolyses constants, Ziemniak et al. (1993) extracted the ΔH_f^0 and S^0 at 25°C for $Ti(OH)_4^0$ and $Ti(OH)_5^-$ as -1515.28 and -1733.8628 kJ mol^{-1}, and 21.6 and 103 J mol^{-1} K^{-1}, respectively.

In the present study, the HKF equation-of-state parameters for aqueous $Ti(OH)_4^0$ were regressed from the experimental results of Ziemniak et al. (1993) and the correlations given by Shock and Helgeson (1988) and Shock et al. (1997). This was done in a similar manner to $H_4SiO_4^0$. The $\Delta\overline{G}^0$ of $Ti(OH)_4^0$ was calculated from 20°C to 290°C from the reaction

$$TiO_{2,\text{rutile}} + 2H_2O = Ti(OH)_4^0$$

according to $\Delta G_r^0 = 1120 + 168.67 \times T$ (Ziemniak et al., 1993) and the thermodynamic properties of rutile (Robie and Hemingway, 1995) and water

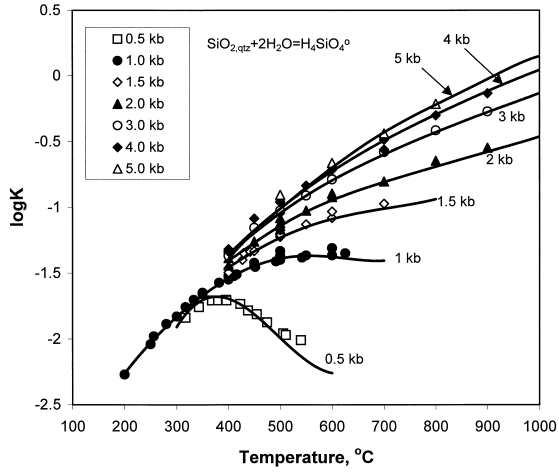

Fig. 4. Logarithm of the solubility constant (log K) for quartz in pure water at elevated temperatures and pressures. The symbols represents experimental data (see text). The curves were calculated using the thermodynamic properties and HKF equation-of-state parameters of aqueous silica obtained in the present study combined with data on quartz (Helgeson et al., 1978) and water (SUPCRT92).

(SUPCRT92). These values were then fitted using a linear least square method to obtain the values for S^0, c_1, c_2 and ω. The partial molal volume (V^0) was estimated from correlation between S^0 and V^0 given by Shock et al. (1997). Further, the a_1, a_2, a_3 and a_4 equation-of-state parameters in the HKF model were calculated from this estimated V^0 value from the correlation algorithms given by Shock and Helgeson (1988). The results are given in Table 3.

The standard absolute entropy of $Ti(OH)_4^0$ at 25°C of 21.92 J mol^{-1} K^{-1} obtained in the present study is almost identical to the S^0 value reported by Ziemniak et al. (1993). Further, the calculated $\Delta\overline{G}^0$ values using the HKF equation-of-state parameters assessed in the present study are within ± 500 J mol^{-1} of the original results, which is well within the errors given by Ziemniak et al. (1993).

5. Thermodynamics of end-member minerals of basalt

The selected thermodynamic data for end-member basaltic minerals are summarized in Table 4. For all the minerals, except end-member plagioclases, the thermodynamic database of Robie and Hemingway (1995) was selected. The reason for selecting this database instead of, e.g. that of Berman (1988), was that it is consistent with the thermodynamic properties of $Fe(OH)_4^-$ and $Ti(OH)_4^0$ derived from hematite and rutile solubility experiments, respectively, and closely matches the data used to derive thermodynamic properties of aqueous $H_4SiO_4^0$ and $Al(OH)_4^-$ extracted from solubility experiments for quartz and Al-bearing minerals (gibbsite, boehmite and diaspore), respectively. In addition, the database of Robie and Hemingway (1995) contained data on all the end-member minerals of interest in the present study.

Arnórsson and Stefánsson (1999) reviewed data on the thermodynamic properties of end-member feldspar minerals and evaluated a solid solution model for calculating thermodynamic properties of plagioclases and alkali feldspars of different composition and Si–Al ordering. In the present study, the solution model of Arnórsson and Stefánsson (1999) was used to calculate the thermodynamic properties of plagioclase solid solutions of fixed composition. As such, their recommended thermodynamic properties of end-member feldspars have been selected here, since they are consistent with the solution model used.

6. Basaltic mineral solid solutions

Gíslason and Arnórsson (1990, 1993) expressed the standard state of mineral solid solutions as an ideal solution of fixed composition at the temperature and pressure of interest. This definition was considered convenient for studying the saturation state of primary basaltic minerals in natural waters, whether the solution is ideal or not. It requires assessment of the thermodynamic properties of a solid solution of a given composition at 25°C and 1 bar, estimated from solution models, taking into account non-ideal behavior and ordering–disordering as appropriate, as well as a heat capacity–temperature equation for that solution.

The specific composition of the solid solutions selected here were those of the average primary basaltic mineral compositions found in basaltic rocks in Iceland, as given by Gíslason and Arnórsson (1990, 1993), based on data from Carmichael (1967) and Fisk (1978).

The apparent standard partial molal Gibbs energy and entropy of a solution at any temperature is given by

$$\Delta\overline{G}^0_{ss} = \sum_i X_i \Delta\overline{G}^0_i - TS^{conf} + G^{ex} \quad (6)$$

and

$$S^0_{ss} = \sum_i X_i S^0_i + S^{conf} + S^{ex} \quad (7)$$

where $\Delta\overline{G}^0_i$, S^0_i and X_i denote the apparent standard partial molal Gibbs energy, the conventional third law entropy and mole fraction of the i-th end-member, respectively, and G^{ex} and S^{ex} are the Gibbs energy and entropy of excess, respectively. The configurational entropy, S^{conf}, is defined as

$$S^{conf} = -R\sum_j n_j \sum_e X_{e,j} \ln X_{e,j} \quad (8)$$

where n_j is the number of times the constituent appears in the formula in the j-th site and $X_{e,j}$ is the mole fraction of the e-th ion in the j-th site.

The excess Gibbs energy of mixing can be resolved into contribution from excess enthalpy, excess entropy and excess volume, i.e.

$$G^{ex} = H^{ex} - TS^{ex} + V^{ex}(P-1) \quad (9)$$

In the present study, the heat capacity of mixing was taken to be zero. Therefore, the heat capacity of a solid solution of fixed composition may be derived by adding up the heat capacities of its end-member minerals in the appropriate proportions, or

$$C^0_{p,ss} = \sum_i X_i C^0_{p,i} \quad (10)$$

The above equations form the basis for estimating the thermodynamic properties of the basaltic mineral solid solutions discussed below.

6.1. Olivine

Olivine forms a binary solid solution between forsterite (Mg_2SiO_4) and fayalite (Fe_2SiO_4). The mixing properties of olivine have been described by asymmetric solid solution models (e.g., Wood and Kleppa, 1981). Sack and Ghiorso (1989) found that the available calorimetric and phase equilibrium data were better described with a symmetric regular solution parameter (W^H) equal to 10.17 kJ mol^{-1}, indicating a large deviation of olivine solid solution from ideality. More recent studies do not support the results of Sack and Ghiorso (1989), and values in the range 3–5 kJ mol^{-1} for W^H, and an excess entropy of less than 2 kJ mol^{-1} K^{-1} have been suggested (Hackler and Wood, 1989; Wiser and Wood, 1991; von Seckendorff and O'Neill, 1993; Kojitani and Akaogi, 1994; Berman et al., 1995; Berman and Aranovich, 1996). Using these values, results in excess Gibbs energy of 0–1500 J mol^{-1}, which corresponds to up to 0.5 log K higher solubility of olivine solid solution in the range 0–350°C than would be predicted if olivine behaved ideally. Torgeson and Sahama (1948) measured the heat of solution of a suite of olivine solid solutions by acid calorimetry around 75°C. Their results are consistent with the observation of olivine solid solution being close to ideal at this temperature.

There are two crystallographic sites, M1 and M2, in olivine. Cation ordering between these sites could result in a configurational enthalpy, entropy and heat capacity for olivine. However, Fe^{2+} and Mg^{2+} appear to be almost randomly distributed between the two types of crystallographic sites (e.g., Ottonello et al., 1990), suggesting that ΔC_p^{mix} is zero. This allows the extrapolation of the interaction parameters, which are based on mixing properties of olivine at

Table 5
Interaction parameters for primary mineral solid solutions used in the present study

Phase	Formula	Site	W_H (J mol^{-1})	W_S (J mol^{-1} K^{-1})	Ref.
Olivine	$(Mg,Fe)_2SiO4$		10,366.2	4	[a]
Orthopyroxene	$(Mg,Fe)SiO_3$		−2600.4	−1.34	[a]
Clinopyroxene	$(Mg,Fe)SiO_3$	M1	−1910	−1.05	[b]
Clinopyroxene	$(Ca,Mg,Fe)SiO_3$	M2	0	0	[b]
Plagioclase	$(Na,Ca)(Al,Si)Si_2O_6$		0	0	[c]
Ilmenite–hematite	$(Fe^{2+},Fe^{3+})(Fe^{2+},Fe^{3+},Ti)O_3$	hi	44,204.8	12.2744	[d]
	$(Fe^{2+},Fe^{3+})(Fe^{2+},Fe^{3+},Ti)O_3$	ih	126,342.5	100.6	[d]
Ulvöspinel–magnetite	$(Fe^{2+},Fe^{3+})(Fe^{2+},Fe^{3+},Ti)O_4$	mu	15,748.03	0	[d]
	$(Fe^{2+},Fe^{3+})(Fe^{2+},Fe^{3+},Ti)O_4$	um	46,175.48	23.0765	[d]

[a] Berman and Aranovich (1996).
[b] Berman et al. (1995).
[c] Arnórsson and Stefánsson (1999).
[d] Anderson and Lindslay (1988).

elevated temperatures, to the temperature regime of interest in this study (0–350°C). On the basis of this, the thermodynamic properties of olivine solid solution of fixed composition were calculated using the interaction parameters of Berman and Aranovich (1996) (Table 5). Their interaction parameters were selected as these parameters are consistent with many other solid solutions in the system FeO–MgO–CaO–Al_2O_3–TiO_2–SiO_2. However, very similar results of olivine solubility would have been obtained if the interaction parameters given by Hackler and Wood (1989), Wiser and Wood (1991), von Seckendorff and O'Neill (1993), Kojitani and Akaogi (1994) or Berman et al. (1995) had been used.

6.2. Pyroxenes

In its simplest form, ignoring all impurities and Ca substitution, orthopyroxene is a binary solid solution between orthoenstatite ($MgSiO_3$) and ferrosilite ($FeSiO_3$). There are two different crystallographic sites in these pyroxenes on which substitution takes place, M1 and M2. At elevated temperatures, Fe and Mg are randomly distributed between these sites. With decreasing temperatures, however, orthopyroxene becomes increasingly ordered with Fe^{2+} occupying the larger M2 site (e.g., Saxena and Ghose, 1971). Therefore, two-site models with non-convergent ordering of Mg and Fe have been applied to describe the mixing properties of orthopyroxene (e.g., Sack, 1980; Chatillon-Colinet et al., 1983; Sack and Ghiorso, 1989) but one-site models have also been used successfully (Saxena, 1981; Aranovich and Kosyakova, 1987; Lee and Ganguly, 1988).

Berman and Aranovich (1996) observed that a one-site model, which is equivalent to a two-site model with complete Fe–Mg disorder between M1 and M2 sites, with symmetric, temperature-dependent excess Gibbs energy reproduced the overall set of experimental observation, when considering mixing of some minerals in the system FeO–MgO–CaO–Al_2O_3–TiO_2–SiO_2, more closely than the two-site model. Extrapolation of this model to temperatures below 400°C results in a smaller departure from ideality than the two-site model of Sack (1980) and Sack and Ghiorso (1989). The one-site model is, however, unable to produce the two immiscibility gaps suggested by Sack (1980) and Sack and Ghiorso (1989) at low temperatures as a result of ordering.

As Mg–Fe order–disorder affects the thermodynamic properties of orthopyroxene, it also influences their solubility, making ordered orthopyroxenes less soluble than disordered ones. It is, however, not known whether orthopyroxene, which always form at high temperatures, attain equilibrium ordering at low temperatures; the rate of such an ordering process is also unknown. The thermodynamic properties of ordered and disordered orthopyroxene may be obtained from data given by von Seckendorff and O'Neill (1993), who measured the solution properties of orthopyroxene at high temperatures where orthopyroxene can be regarded as fully disordered, and solution modeling proposed by Sack and Ghiorso (1989). The difference between the solubility of fully ordered and fully disordered $En_{38}Fs_{62}$, which is the orthopyroxene composition of interest in the present study, is equivalent to 0.5 log K units at 25°C and it decreases with increasing temperature. Using the simple one-site model and the interaction parameters of Berman and Aranovich (1996) results in a solubility that is intermediate between these two. For this reason, and because of its simplicity and its consistency with the interaction parameters of olivine selected in this study, the thermodynamic properties of orthopyroxene of composition $En_{38}Fs_{62}$ have been assessed using a one-site model and the interaction parameters given by Berman and Aranovich (1996) (Table 5).

Ignoring Al and Na substitution and impurities, clinopyroxene is a complex multi-component and multi-site solution with mixing of Ca, Fe, and Mg between M1 and M2 sites. Site occupancy data for clinopyroxene show a strong partitioning of Fe into the M2 site. Also, Ca almost entirely occupies the M2 site. However, considerable uncertainties remain in predicting Mg–Fe occupancy, particularly with respect to temperature and Ca content. These uncertainties can be clearly seen from the disagreement between site occupancies measured experimentally and those calculated by applying non-convergent ordering model parameters derived from phase equilibria (Brown et al., 1972; Saxena et al., 1974; McCallister et al., 1976; Davidson and Lindsley 1985; Sack and Ghiorso, 1994a,b). On the basis of this, Berman et al. (1995) concluded that ordering

models were not supported by site occupancy data over wide temperature and composition ranges.

The purpose of the present study is to evaluate the mineral solubility from 0°C to 350°C, which is far from the temperature conditions where clinopyroxene solution model parameters have been constructed. As it is uncertain whether natural clinopyroxene reacting with natural waters has attained equilibrium ordering with respect to the temperature of the system, or if the ordering is "frozen in" at the formation temperature, a very simplified model has been adopted for calculating the thermodynamics of clinopyroxene solid solution of fixed composition. The model treats the M1 site as an ideal binary solution of Mg and Fe and the M2 site as an ideal ternary solution of Ca, Fe and Mg. The ratio $Mg/(Mg + Fe)$ is further assumed to be equal in both sites. In this context, it is important to note that large uncertainties are involved in estimating the thermodynamic properties of the clinopyroxene solid solutions at low temperatures and, therefore, their estimated solubilities. This should be kept in mind when interpreting the saturation state of these minerals in a natural water of a specific composition.

6.3. Plagioclase feldspars

Newton et al. (1980) and Carpenter et al. (1985) determined the heat of solution of plagioclase feldspars of various compositions. Their results are consistent with the interpretation that plagioclase forms two ideal solid solutions, a "high" and "low" temperature series, respectively. The high series represents heat-treated and, therefore, disordered structure, whereas the "low" series represents natural plagioclases from metamorphic and plutonic rocks. The latter are in all likelihood partly disordered. Each series is composed of two segments one for An_0–An_{70} and the other for An_{70}–An_{100}. The "high" series involves a transformation from $C\bar{1}$ to "high" $I\bar{1}$ symmetry and the "low" series from "e" to "low" I1 symmetry. These transformations have considerable effects on the thermodynamic properties of plagioclase feldspars.

Arnórsson and Stefánsson (1999) estimated the enthalpy, entropy and Gibbs energy of the albite and anorthite components in both segments of the "high" and "low" plagioclase series permitting evaluation of the thermodynamic properties of plagioclase of any composition in both series (Table 4). Their solution model has been used in the present study to evaluate the solubility of intermediate plagioclases of composition $An_{70}Ab_{30}$ and $An_{29}Ab_{71}$ for the "high" plagioclase series.

There is a lack of information on the degree of ordering with respect to Al–Si and Na–Ca in plagioclases from volcanic rocks. It is not known to what extent the ordering is frozen in from the formation temperature. It appears logical that plagioclases in volcanic rock are less ordered than those in deep-seated metamorphic and plutonic rocks (the "low" series). Probably they are intermediate between the two series. This contribution is mainly concerned with studying the saturation state of natural waters with naturally occurring primary plagioclases in volcanic rocks in Iceland, which formed at high temperatures and are of Quaternary and Tertiary age. They are therefore assumed to be largely disordered.

6.4. Magnetite–ulvöspinel and hematite–ilmenite

Fe–Ti oxides are important constituents of igneous rocks. In this contribution two solid solutions were considered, hematite–ilmenite and magnetite–ulvöspinel. Both show a complete solid solution at high temperature but immiscibility gaps are recognized at low temperatures (Deer et al., 1992). However, despite the great importance of these minerals to the geological sciences, their cation distribution and solid solution thermodynamics are poorly understood.

Two different approaches have been taken to model spinel solid solutions. They are microscopic formulations (e.g., O'Neill and Navrotsky, 1984; Sack and Ghiorso, 1991), and the macroscopic models of Sack (1982) and Anderson and Lindsley (1988), which quite successfully reproduce the macroscopic properties of magnetite–ulvöspinel solid solutions. However, the macroscopic models are not consistent with the results of Wu and Mason (1981), Trestman-Matts et al. (1983), O'Neill and Navrotsky (1983, 1984) for cation ordering between tetrahedral and octahedral sites in the spinel structure. Yet, because of its simplicity and its ability to reproduce

Table 6
Thermodynamic properties of primary mineral solid solutions of selected composition at 25°C and 1 bar

Mineral	Formula	$\Delta G^0_{r,T_r}$ (kJ mol^{-1})	$\Delta H^{0a}_{f,T_r}$ (mJ mol^{-1})	$S^0_{T_r}$ (J mol^{-1} K^{-1})	$V^0_{T_r}$ (cm^3 mol^{-1})	$C^0_{P_r} = a + bT + cT^{-2} + fT^2 + gT^{-0.5}$				
						$a \times 10^{-2}$ (J mol^{-1})	$b \times 10^2$ (J mol^{-1} K^{-2})	$c \times 10^{-6}$ (J K mol^{-1})	$f \times 10^5$ (J mol^{-1} K^{-3})	$g \times 10^{-3}$ (J mol^{-1} K$^{-0.5}$)
Olivine	$Fo_{80}Fa_{20}$	−1919.7	−2022.9	114.4	44.18	1.0509	6.797	−3.737	−1.295	0.6749
Olivine	$Fo_{43}Fa_{57}$	−1670.3	−1765.8	138.9	45.17	1.3790	3.246	−3.807	0.447	0.3627
Orthopyroxene	$En_{58}Fs_{82}$	−1249.5	−1322.4	89.1	32.36	2.103	−4.69	−1.422	2.214	−1.632
Clinopyroxene	$Di_{45}Hed_{25}En_{19}Fs_{11}$	−2835.3	−2888.5	166.3	65.78	3.947	−4.291	−0.641	1.266	−3.554
Plagioclase	$An_{70}Ab_{30}$	−3906.5	−4108.2	217.9	100.8	5.632	−10.875	−0.033	4.029	−5.605
Plagioclase	$An_{29}Ab_{71}$	−3788.5	−3988.3	225.2	100.8	6.266	−13.098	1.845	3.812	−6.992
Magnetite	$Mt_{15}Usp_{85}$	−1341.5	−1423.8	193.8	46.48	3.117	−25.71	−4.663	20.52	−0.988
Magnetite	$Mt_{68}Usp_{32}$	−1132.8	−1218.7	179.0	45.256	17.754	−166.90	11.173	93.00	−23.103
Hematite	Hem_7Ilm_{93}	−1125.4	−1225.4	101.9	31.59	3.494	−15.94	1.345	7.134	−3.865

[a]Calculated from the ΔG^0_f and S^0 values in the table together with S^0 for the elements given by Cox et al. (1989).

Table 7
Logarithms of the dissociation of dissolution reaction listed in Table 1 at temperature ranging from 0°C to 350°C and saturated water vapour pressure calculated with thermodynamic properties of aqueous species and minerals given in Tables 2–4 and 6)

Mineral	Composition	0	25	50	75	100	125	150	175	200	225	250	275	300	325	350
Olivine	Fo_{100}	32.12	28.67	25.71	23.17	20.99	19.08	17.40	15.91	14.56	13.34	12.20	11.12	10.11	9.17	8.39
	Fa_{100}	22.43	19.83	17.57	15.63	13.95	12.47	11.16	9.99	8.92	7.94	7.02	6.14	5.30	4.50	3.83
	$Fo_{80}Fa_{20}$	30.03	26.72	23.88	21.45	19.34	17.51	15.89	14.45	13.15	11.97	10.86	9.82	8.83	7.91	7.15
	$Fo_{43}Fa_{53}$	26.43	23.42	20.83	18.61	16.68	15.00	13.51	12.18	10.98	9.88	8.85	7.88	6.95	6.08	5.36
Pyroxene	En_{100}	13.33	11.87	10.59	9.49	8.54	7.71	6.97	6.32	5.73	5.19	4.69	4.22	3.76	3.34	2.98
	Fs_{100}	9.06	7.99	7.02	6.18	5.45	4.80	4.22	3.71	3.24	2.80	2.39	1.99	1.60	1.23	0.91
	Di_{100}	12.07	10.87	9.82	8.90	8.10	7.41	6.79	6.24	5.74	5.28	4.85	4.44	4.04	3.66	3.32
	Hed_{100}	10.92	9.82	8.85	8.00	7.26	6.60	6.02	5.50	5.03	4.59	4.18	3.79	3.40	3.03	2.70
	$En_{38}Fs_{62}$	10.29	9.08	8.00	7.07	6.26	5.55	4.92	4.35	3.84	3.37	2.93	2.50	2.09	1.70	1.37
	$Di_{45}Hed_{25}En_{19}Fs_{11}$	11.68	10.45	9.35	8.41	7.58	6.86	6.23	5.66	5.14	4.67	4.22	3.80	3.38	2.99	2.65
Plagioclase	An_{100}	−21.43	−20.46	−19.82	−19.37	−19.04	−18.82	−18.67	−18.61	−18.62	−18.71	−18.90	−19.20	−19.64	−20.24	−21.15
	Ab_{100}	−20.39	−18.77	−17.57	−16.62	−15.82	−15.14	−14.55	−14.05	−13.63	−13.27	−13.00	−12.80	−12.71	−12.74	−12.98
	$An_{70}Ab_{30}$	−19.82	−18.82	−18.14	−17.65	−17.28	−17.01	−16.81	−16.68	−16.62	−16.63	−16.73	−16.93	−17.24	−17.71	−18.45
	$An_{29}Ab_{71}$	−20.14	−18.80	−17.83	−17.08	−16.46	−15.96	−15.54	−15.20	−14.94	−14.74	−14.62	−14.60	−14.68	−14.89	−15.35
	Mt_{100}	−32.65	−31.51	−30.65	−29.94	−29.32	−28.78	−28.30	−27.89	−27.53	−27.24	−27.02	−26.90	−26.89	−27.01	−27.42
Magnetite–ulvospinel	Usp_{100}	20.04	16.75	13.96	11.57	9.51	7.70	6.10	4.67	3.37	2.17	1.06	0.01	−1.00	−1.93	−2.72
	$Mt_{15}Usp_{85}$	12.29	9.56	7.24	5.25	3.53	2.03	0.69	−0.50	−1.59	−2.59	−3.54	−4.44	−5.32	−6.15	−6.90
	$Mt_{68}Usp_{32}$	−14.96	−15.40	−15.85	−16.25	−16.60	−16.90	−17.16	−17.41	−17.65	−17.89	−18.15	−18.45	−18.81	−19.23	−19.80
	Hem_{100}	−44.65	−42.09	−40.03	−38.29	−36.79	−35.47	−34.29	−33.26	−32.33	−31.52	−30.81	−30.23	−29.77	−29.48	−29.54
Hematite–Ilmenite	Ilm_{100}	3.41	1.98	0.77	−0.27	−1.17	−1.96	−2.65	−3.28	−3.85	−4.37	−4.87	−5.34	−5.79	−6.21	−6.57
	Hem_7Ilm_{93}	0.28	−0.87	−1.85	−2.69	−3.42	−4.06	−4.62	−5.13	−5.59	−6.02	−6.43	−6.82	−7.21	−7.58	−7.92
Apatite	F-Ap_{100}	−30.34	−30.94	−31.92	−33.13	−34.48	−35.96	−37.57	−39.30	−41.18	−43.24	−45.52	−48.12	−51.10	−54.56	−58.88
	OH-Ap_{100}	−24.97	−26.01	−27.38	−28.92	−30.57	−32.32	−34.17	−36.12	−38.19	−40.43	−42.88	−45.62	−48.74	−52.33	−56.78

reasonably well the macroscopic properties of magnetite–ulvöspinel solid solutions the solution model of Anderson and Lindsley (1988) has been selected here (Table 5). This model assumes that Ti^{4+} occupies octahedral sites only and always replaces Fe^{3+} in these sites (Akimoto, 1954), i.e. the structural formula of titanomagnetite solid solution is $(Fe^{2+}_x Fe^{3+}_{1-x})[Fe^{2+} Fe^{3+}_{1-x} Ti_x]O_4$.

Pure hematite has the disordered $R\bar{3}c$ structure whereas pure ilmenite has the ordered $R\bar{3}$ structure. When studying the solution properties of ilmenite–hematite solid solution Spencer and Lindsley (1981) and Anderson and Lindsley (1988) only considered ordered minerals ($R\bar{3}$ structure). Ghiorso (1990) pointed out that the thermodynamic modeling involving hematite–ilmenite solid solution must account for the $R\bar{3}$–$R\bar{3}c$ ordering–disordering transition. Ghiorso (1990) further argued that the excess entropy proposed by Anderson and Lindsley (1988) was unrealistically high compared to the entropies of the end-member hematite and ilmenite. The interest of the present study is to evaluate the solubility of $Ilm_{93}Hem_7$ solid solution in the temperature range 0–350°C. This is the average composition of ilmenite–hematite minerals in Icelandic basalts (Carmichael, 1967). For this composition, ilmenite–hematite solid solution was assumed to be ordered, and that any excess entropy would have little effect on its solution thermodynamics. In fact, the difference in the Gibbs energy of mixing using the procedure of Anderson and Lindsley (1988) and Ghiorso (1990) for $Ilm_{93}Hem_7$ assuming total ordering is 1200 J at 25°C. This difference is trivial when calculating $Ilm_{93}Hem_7$ solubility in comparison with the uncertainties in the thermodynamic values for the aqueous titanium hydroxy complexes. As it is consistent with the solution model selected for magnetite–ulvöspinel, the thermodynamic properties of $Ilm_{93}Hem_7$ have been calculated using the interaction parameters of Anderson and Lindsley (1988) (Table 5).

7. Basaltic mineral solubility

The logarithms of the solubility constants for primary basaltic minerals (Table 1) were calculated from the apparent standard Gibbs energies of the minerals and the respective aqueous species Tables 2–4 and 6) using Eqs. (1)–(5). The results are given in Table 7 and compared with previous results in Figs. 5 and 6.

The apparent standard Gibbs energy of the aqueous species and water was calculated with the aid of the SUPCRT92 code (Johnson et al., 1992), which was modified in the present study to include the thermodynamic properties and HKF equation-of-state parameters for $Al(OH)^-_4$ ($AlO^-_2 + 2H_2O$) (Pokrovskii and Helgeson, 1995), $Fe(OH)^-_4$ (Diakonov et al., 1999) and $H_4SiO^0_4$ and $Ti(OH)^0_4$ estimated in the present study.

8. Discussion and conclusions

In the present study, the solubilities of olivine, plagioclase, orthopyroxene, clinopyroxene and Fe–Ti oxides have been retrieved, both for end-member minerals and solid solutions of fixed composition. This should be of value for the study of the dissolution of all the primary basaltic minerals of natural composition in natural waters. It seems unlikely that improved solution modeling for olivine will change its calculated solubility to a significant degree. The same is true for orthopyroxene, even though large uncertainties are related to cation distribution. This is related to small differences in solubilities between ordered and disordered orthopyroxene. However, improved modeling of clinopyroxene, especially related to cation distribution at low temperatures, may have significant influence on calculated clinopyroxene solubility. Also, the solubilities of naturally occurring Fe–Ti oxides may be improved data on the Ti end-member and by better understanding their solid solution behaviour.

The solubilities of end-member primary silicate and non-silicate basaltic minerals derived in this study are plotted in Figs. 5 and 6. They are compared with previously published solubilities reported by Bowers et al. (1984) and calculated using the SUPCRT92 code (Johnson et al., 1992) using the most recent database (slop98.dat). The solubilities of apatite have been compared with those reported in the SOLMINEQ88 program (Kharaka et al., 1988).

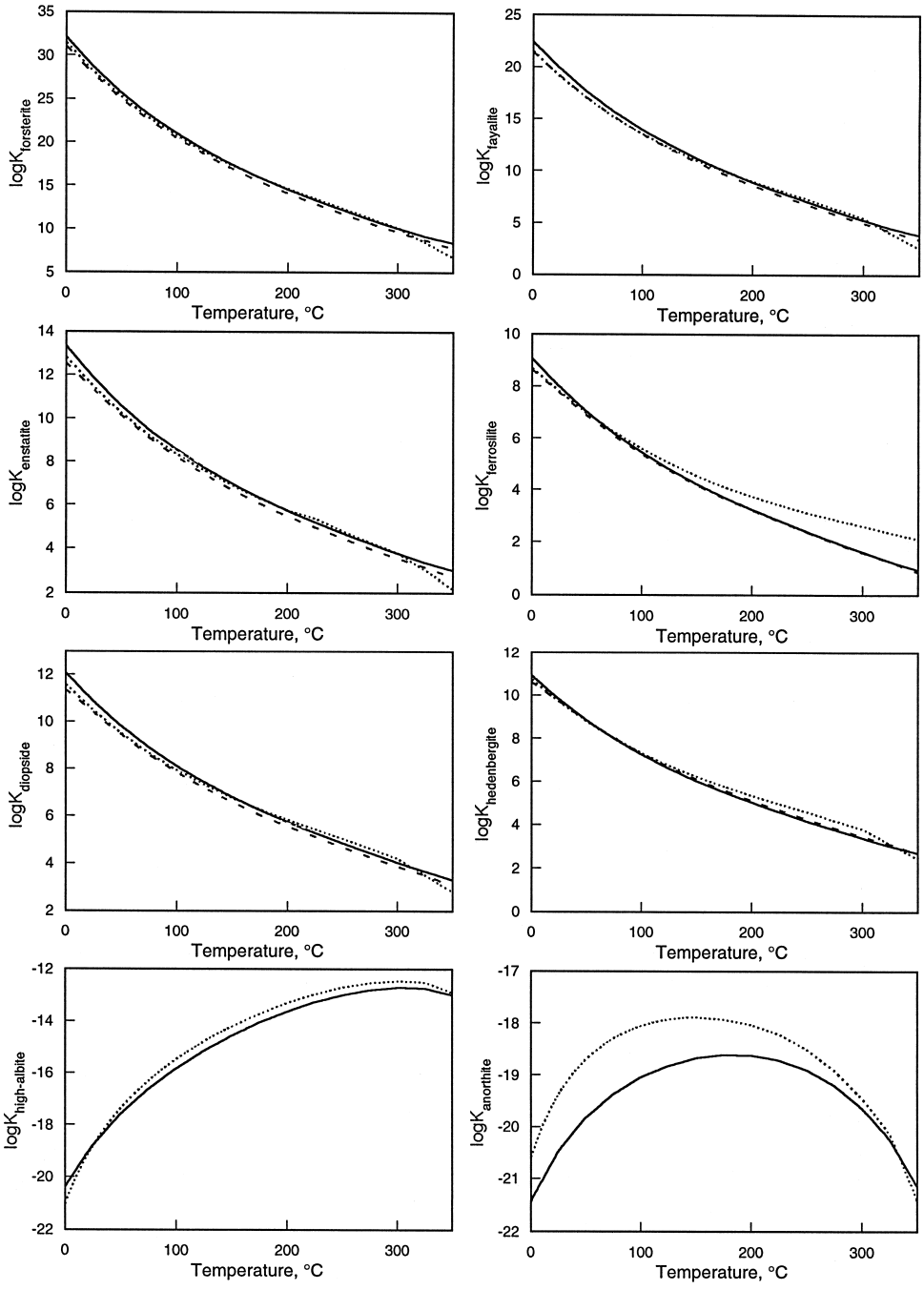

Fig. 5. Comparison between the solubility of end-member primary silicate minerals of basalt. Solid line, this study; dotted line, Bowers et al. (1984); broken line, SUPCRT92 (Johnson et al., 1992).

Above 100°C, the results of the present study and SUPCRT92 are similar for forsterite, fayalite, enstatite, ferrosilite, and diopside. The same is true for the solubilities reported by Bowers et al. (1984),

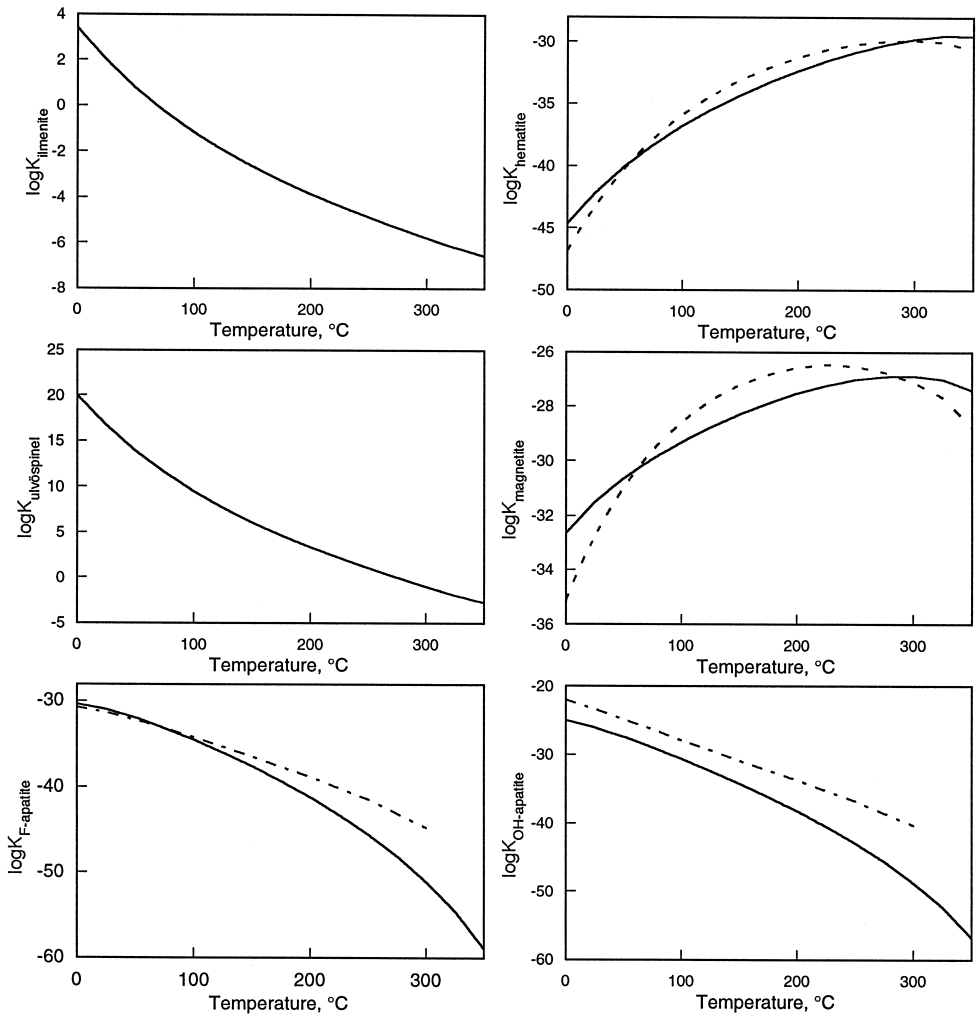

Fig. 6. Comparison between the solubility of end-member primary non-silicate minerals of basalt. Solid line, this study; broken line, SUPCRT92 (Johnson et al., 1992); dotted-line SOLMINEQ88 (Kharaka et al., 1988).

except for ferrosilite. On the other hand higher solubilities are observed in the present contribution below 100°C and particularly below 50°C for all the silicate minerals than hitherto reported. For high-albite and anorthite, a somewhat different trend is observed. The Gibbs energy of anorthite and high-albite used in the SUPCRT92 program (Helgeson et al., 1978) at 25°C is less negative by 10 and 4 kJ mol^{-1}, respectively, than those used in the present study. However, this difference is partially overshadowed by the different thermodynamic properties of $H_4SiO_4^0$ of the present study and those reported by Shock and Helgeson (1988), which are used in the SUPCRT92 code, leading to relatively similar solubility constants, especially for high-albite. It should, however, be noted that this is a pure coincidence as the thermodynamic properties for aqueous silica and the minerals used in SUPCRT92 are thought to be in error. Also, considerable differences are observed for hematite and magnetite solubilities.

The solubility curves obtained in this study for the olivine, plagioclase and orthopyroxene solid solu-

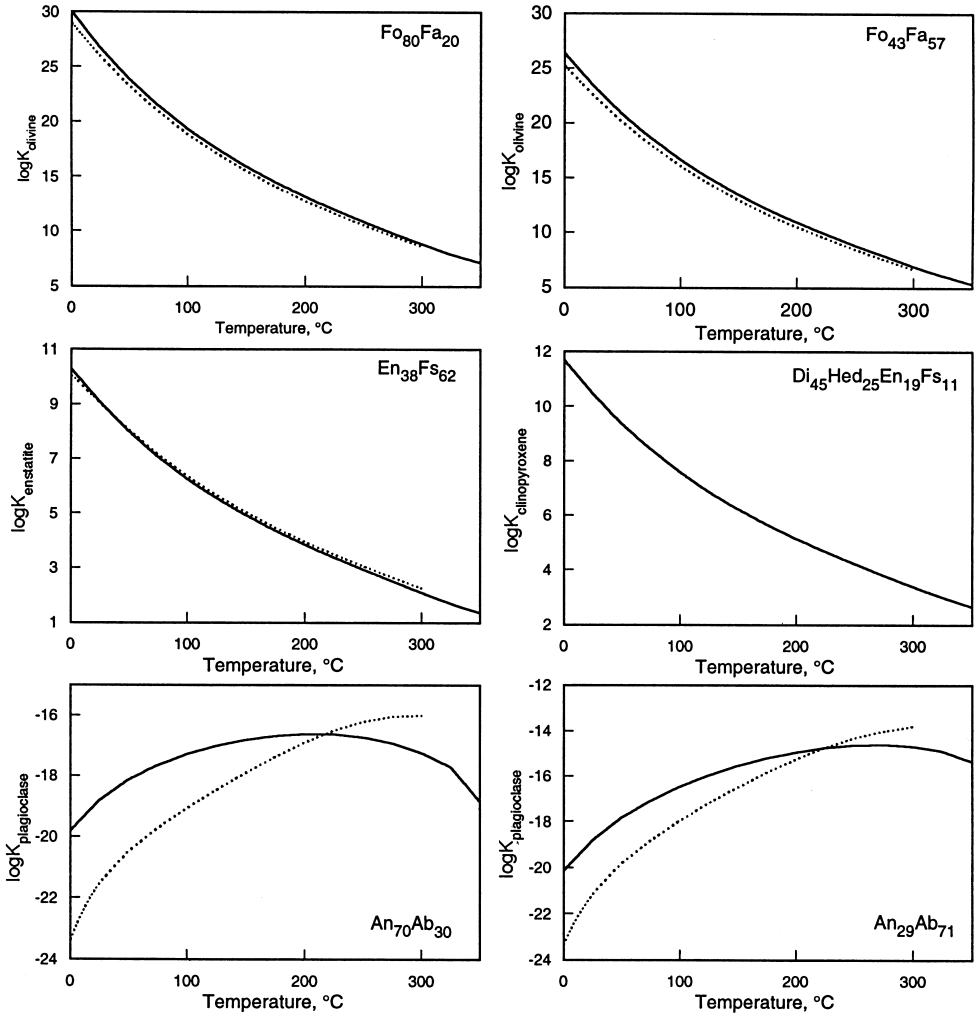

Fig. 7. The solubility of primary silicate basaltic mineral solid solutions of fixed composition. Solid line, this study; dotted-line, Gíslason and Arnórsson (1993).

tions are compared with the earlier results of Gíslason and Arnórsson (1990, 1993) in Fig. 7. In Fig. 8, the solubility for hematite–ilmenite and magnetite–ulvöspinel solid solutions estimated in the present study are shown. Results of the present study indicate higher solubilities of olivine, but they are similar for orthopyroxene, except below 100°C. Higher solubility is obtained for plagioclase solid solution, the difference being about three orders of magnitude at 25°C.

The difference in the solubility of silicate-bearing minerals below 100°C lies primarily in the thermodynamic data obtained in the present study for aqueous $H_4SiO_4^0$, which is based on recent experimental results on quartz and amorphous silica solubilities (Rimstidt, 1997; Gunnarsson and Arnórsson, 2000). Additionally, the differences in the plagioclase and olivine solid solution solubilities are attributed to different solid solution models used in the present study. The difference between the solubilities for

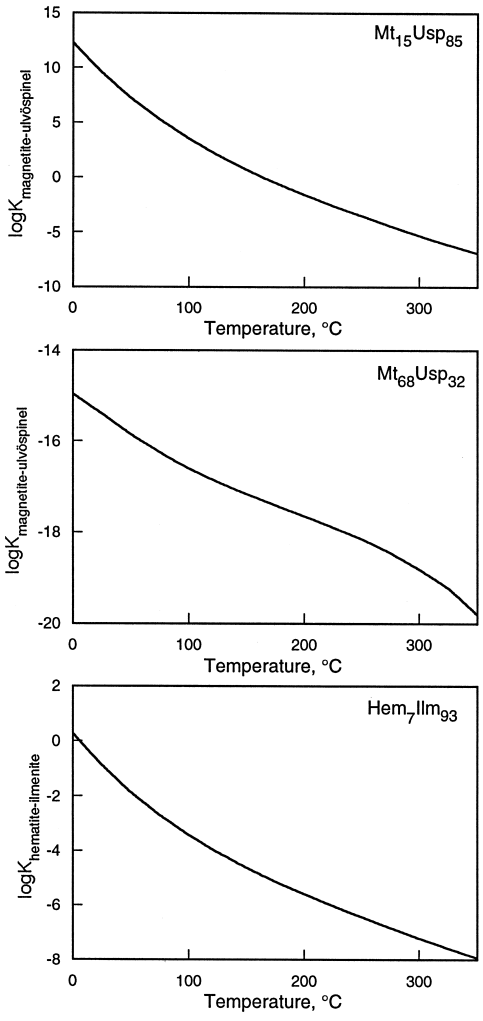

Fig. 8. The solubility of primary non-silicate basaltic mineral solid solutions of fixed composition estimated in the present study.

hematite and magnetite presented in this study, on one hand, and of SUPCRT92, on the other, lie in the thermodynamic properties $Fe(OH)_4^-$. The data on $Fe(OH)_4^-$ ($FeO_2^- + H_2O$) by Shock et al. (1997), which are used in SUPCRT92, are based on solubility of amorphous iron hydroxide and empirical correlations, and do not match well with experimental results on hematite solubility and are considered to be erroneous (Diakonov et al., 1999).

The solubilities obtained in the present study may be used to gain a better understanding of the geochemical processes of great importance. For example, the oceanic floor is largely made of basaltic rocks, the dissolution of which is important for the oceanic chemistry and the CO_2 budget of the ocean. Also, dissolution of apatite is a major source of phosphorous in surface environments, which is an essential nutrient for organic activity. Further, feldspar minerals are the most abundant group of minerals of the Earth's crust and are an important source for Ca, Na, Al and Si in natural waters. Also, the greater solubilities for most minerals reported in the present contribution below 100°C have a large effect on the interpretation of the behaviour of these minerals under weathering conditions. Comparison of these solubilities with calculated reaction quotients for natural waters will be the scope of another contribution (Stefánsson et al., 2000).

Acknowledgements

The present study was supported by the Student Fund of the National Research Council, Iceland, and Icelandic Alloys. I am indebted to S. Arnórsson and S.R. Gíslason for their assistance and fruitful discussions during the course of this work. Reviews by I. Diakonov and that of an anonymous reviewer greatly improved the manuscript and are sincerely appreciated.

References

Akimoto, S., 1954. Thermo-magnetic study of ferromagnetic minerals contained in igneous rocks. J. Geomagn. Geoelectr. 6, 1–14.

Anderson, G.M., Burnham, C.W., 1965. The solubility of quartz in supercritical steam. Am. J. Sci. 263, 494–511.

Anderson, G.M., Burnham, C.W., 1967. Reactions to quartz and corundum with aqueous chloride and hydroxide solutions at high temperatures and pressures. Am. J. Sci. 265, 12–27.

Anderson, D.J., Lindsley, D.H., 1988. Internally consistent solution models for Fe–Mg–Mn–Ti oxides: Fe–Ti oxides. Am. Mineral. 73, 714–726.

Apps, J.A., Neil, J.M., Jun, C.H., 1989. Thermochemical Properties of Gibbsite, Bayerite, Boehmite, Diaspore, and the Aluminate Ion Between 0 and 350°C. Div. Waste Mgt., Office of

Nucl. Material Safety and Safeguards, US NRC NUREC/CR-5271-LBL 21482.

Aranovich, L.Y., Kosyakova, N.A., 1987. The cordierite = orthopyroxene + quartz equilibrium: laboratory data on and thermodynamics of ternary Fe–Mg–Al orthopyroxene solid solutions. Geochim. Int. 24, 111–131.

Arnórsson, S., Andrésdóttir, A., 1999. The dissociation constants of Al-hydroxy complexes at 0–350°C and Psat. In: Ármannsson, H. (Ed.), Chemistry of the Earth's Surfaces: Proceedings of the 5th symposium on Geochemistry of the Earth's surfaces. Balkema, Rotterdam, pp. 425–428.

Arnórsson, S., Stefánsson, A., 1999. Assessment of feldspar solubility constants in water in the range of 0° to 350°C at vapor saturation pressures. Am. J. Sci. 299, 173–209.

Arnórsson, S., Sigurdsson, S., Svavarsson, H., 1982. The chemistry of geothermal waters in Iceland: I. Calculation of aqueous speciation from 0° to 370°C. Geochim. Cosmochim. Acta 46, 1513–1532.

Arnórsson, S., Geirsson, K., Andrésdóttir, A., Sigurdsson, S., 2000. Compilation and evolution of thermodynamic data on the solubility of CO_2, H_2S, H_2, CH_4, N_2, O_2 and Ar in pure water in the range 0–350°C. Am. J. Sci. submitted.

Babko, A.K., Gridchina, G.I., Nabivanets, B.I., 1962. Study of titanium(IV) in hydrochloric acid by dialysis and ion-exchange chromatography. Russ. J. Inorg. Chem. 7, 66–70.

Baes Jr., C.F., Mesmer, R.E., 1976. The Hydrolysis of Cations. Wiley-Interscience, 489 pp.

Baes Jr., C.F., Mesmer, R.E., 1981. The thermodynamics of cation hydrolysis. Am. J. Sci. 281, 935–962.

Berman, R.G., 1988. Internally-consistent thermodynamic data for minerals in the system K_2O–Na_2O–CaO–MgO–FeO–Fe_2O_3–Al_2O_3–SiO_2–TiO_2–H_2O–CO_2: representation, estimation and high temperature extrapolation. Contrib. Mineral. Petrol. 89, 168–183.

Berman, R.G., Aranovich, L.Ya., 1996. Optimized standard state and solution properties of minerals: I. Model calibration for olivine, orthopyroxene, cordierite, garnet, and ilmenite in the system FeO–MgO–CaO–Al_2O_3–TiO_2–SiO_2. Contrib. Mineral. Petrol. 126, 1–24.

Berman, R.G., Aranovich, L.Ya., Pattison, D.R.M., 1995. Reassessment of the garnet-clinopyroxene Fe–Mg exchange thermometer: II. Thermodynamic analysis. Contrib. Mineral. Petrol. 119, 30–42.

Biederman, G., Schindler, P., 1957. On the solubility product of precipitated iron(III) hydroxide. Acta Chem. Scand. 1l, 731–740.

Bjarnason, J.O., 1994. The speciation program WATCH. Icelandic National Energy Authority Report. version 2.1A.

Bowers, T.S., Jackson, K.J., Helgeson, H.C., 1984. Equilibrium Activity Diagrams for Coexisting Minerals and Aqueous Solutions at Pressures and Temperatures to 5 kb and 600°C. Springer-Verlag, 397 pp.

Brady, P.V., Gíslason, S.R., 1997. Seafloor weathering controls on atmospheric CO_2 and global climate. Geochim. Cosmochim. Acta 61, 965–973.

Brown, G.E., Prewitt, C.T., Papike, J.J., Sueno, S., 1972. A comparison of the structures of low and high pigeonite. J. Geophys. Res. 77, 5778–5789.

Byrne, R.H., Kester, D.R., 1976. Solubility of hydrous ferrite oxide and iron speciation in sea water. Mar. Chem. 4, 255–274.

Carmichael, I.S.E., 1967. The mineralogy of Thingmuli, a Tertiary volcano in Eastern Iceland. Am. Mineral. 52, 1815–1841.

Carpenter, M.A., McConnell, J.D.C., Navrotsky, A., 1985. Enthalpies of ordering in plagioclase feldspar solid solution. Geochim. Cosmochim. Acta 49, 947–966.

Castet, S., Dandurand, J.L., Schott, J., Gout, R., 1993. Boehmite solubility and aqueous aluminium speciation in hydrothermal solutions (90–350°C): experimental study and modeling. Geochim. Cosmochim. Acta 57, 4869–4884.

Chatillon-Colinet, C., Newton, R.C., Perkins III, D., Kleppa, O.J., 1983. Thermochemistry of $(Fe^{2+},Mg)SiO_3$ orthopyroxene. Geochim. Cosmochim. Acta 47, 1597–1603.

Couturier, Y., Michard, G., Sarazin, G., 1984. Constantes de formation des complexes hydroxydés de l'aluminium en solution aqueuse de 20 a 70°C. Geochim. Cosmochim. Acta 48, 649–659.

Cox, J.D., Wagman, D.D., Medvedev, V.A., 1989. CODATA Key Values for Thermodynamics. Hemisphere Publication, 271pp.

Crerar, D.A., Anderson, G.M., 1971. Solubility and solvation reactions of quartz in dilute hydrothermal solutions. Chem. Geol. 8, 107–122.

Davidson, P.M., Lindsley, D.H., 1985. Thermodynamic analysis of quadrilateral pyroxenes: Part II. Model calibration from experiments and applications to geothermometry. Contrib. Mineral. Petrol. 80, 88–102.

Deer, W.A., Howie, R.A., Zussman, J., 1992. An Introduction to the Rock-Forming Minerals. 2nd edn. Longmann, 696 pp.

Diakonov, I., Tagirov, B.R., 2000. Iron(III) speciation in aqueous solutions: Part 2. Thermodynamic properties of $Fe(OH)^{2+}$, $Fe(OH)_2^+$ and $Fe(OH)_3^0$ species and solubility of iron(III) oxides, and hydroxides (in preparation).

Diakonov, I., Khodakovsky, I., Schott, J., Sergeeva, E., 1994. Thermodynamic properties of iron oxides and hydroxides. Surface and bulk thermodynamic properties of goethite (α-FeOOH) up to 500 K. Eur. J. Miner. 6, 967–983.

Diakonov, I., Pokrovski, G., Schott, J., Castet, S., Gout, R., 1996. An experimental and computational study of sodium aluminium complexing in crustal fluids. Geochim. Cosmochim. Acta 60, 197–211.

Diakonov, I., Schott, J., Martin, F., Harrichourry, J.-Cl., Escalier, J., 1999. Iron(III) solubility and speciation in aqueous solutions. Experimental study and modelling: Part 1. Hematite solubility from 60 to 300°C in NaOH–NaCl solutions and thermodynamic properties of $Fe(OH)_4^-$ (aq). Geochim. Cosmochim. Acta 63, 2247–2261.

Dillenseger, C., 1995. Modélisation de la dissolution des oxy-hydroxydes d'aluminium et de fer dans une solution 5 M NaOH a 200 et 250°C. Application au procédé ayer de traitment de la bauxite. Unpublished PhD thesis, University of Orléans, France.

Fisk, M.R., 1978. Melting relations and mineral chemistry of Iceland and Reykjanes ridge basalts. Unpublished PhD thesis, University of Rhode Island.

Fournier, R.O., 1960. Solubility of quartz in water in the temperature interval from 25°C to 300°C. Geol. Soc. Am. Bull. 71, 1867–1868.

Ghiorso, M.S., 1990. Thermodynamic properties of hematite–ilmenite–geikelite solid solutions. Contrib. Mineral. Petrol. 140, 645–667.

Gíslason, S., Arnórsson, S., 1990. Saturation state of natural waters in Iceland relative to primary and secondary minerals in basalt. In: Spencer, R.J., Chou, I.-M. (Eds.), Fluid-Mineral Interaction: A Tribute to H.P. Eugster. Geochem. Soc. Spec. Publ. No. 2, pp. 373–393.

Gíslason, S.R., Arnórsson, S., 1993. Dissolution of primary basaltic minerals in natural waters: saturation and kinetics. Chem. Geol. 105, 117–135.

Gíslason, S.R., Arnórsson, S., Ármannsson, H., 1996a. Chemical weathering of basalt in southwest Iceland: effects of runoff, age of rocks and vegetative/glacial cover. Am. J. Sci. 296, 837–907.

Gíslason, S.R., Rose, N.M., Oelkers, E.H., 1996b. Chemical weathering, glaciers and the carbon cycle. In: Bottrell, S.H. (Ed.), Fourth International Symposium on The Geochemistry of the Earth's Surface. Balkema Press, pp. 574–577.

Glynn, P.D., Reardon, E.J., 1990. Solid-solution aqueous-solution equilibria: thermodynamic theory and representation. Am. J. Sci. 290, 164–201.

Gunnarsson, I., Arnórsson, S., 2000. The solubility of amorphous silica in the range 0–350°C and the thermodynamic properties of $H_4SiO_4^0$. Geochim. Cosmochim. Acta, in press.

Hackler, R.T., Wood, B.J., 1989. Experimental determination of Fe and Mg exchange between garnet and olivine and estimation of Fe–Mg mixing properties in garnet. Am. Mineral. 74, 994–999.

Helgeson, H., Aagaard, P., 1985. Activity/composition relations among silicates and aqueous solutions: I. Thermodynamics of intrasite mixing and substitutional order/disorder in minerals. Am. J. Sci. 285, 769–844.

Helgeson, H.C., Delany, J.M., Nesbitt, H.W., Bird, D.K., 1978. Summary and critique of the thermodynamic properties of rock-forming minerals. Am. J. Sci. 278-A, 220 pp.

Helgeson, H.C., Kirkham, D.H., Flowers, G.C., 1981. Theoretical prediction of the thermodynamic behaviour of aqueous electrolytes at high pressures and temperatures: IV. Calculation of activity coefficients, osmotic coefficients, and apparent molal and standard and relative partial molal properties to 600°C and 5 kb. Am. J. Sci. 281, 1249–1516.

Hemley, J.J., Montoya, J.W., Marinenko, J.W., Luce, R.W., 1980. Equilibria in the system Al_2O_3–SiO_2–H_2O and some general implications for alteration/mineralization processes. Econ. Geol. 75, 210–228.

Johnson, J.W., Oelkers, E.H., Helgeson, H.C., 1992. SUPCRT92: A software package for calculating the standard molal properties of minerals, gases, aqueous species and reactions among them from 1 to 5000 bars and 0 to 1000°C. Comp. Geosci. 18, 899–947.

Kamnev, A.A., Ezhov, B.B., Malandin, O.G., Vasev, A.V., 1986. The solubility of goethite in basic solutions. Zh. Prikl. Khim. 8, 1689–1693.

Kennedy, G.C., 1950. A portion of the system silica–water. Econ. Geol. 45, 629–653.

Kharaka, Y.K., Gunter, W.D., Aggarwal, P.K., Perkins, E., DeBraal, J.D., 1988. SOLMINEQ88: a computer program for geochemical modeling of water–rock interactions. U.S. Geol. Surv. Water-Resour. Invest. Rep. 88-4427, 420 pp.

Khitarov, N.I., 1956. The 400°C isotherm for the system H_2O–SiO_2 at pressures up to 2,000 kg/cm^2. Geochemistry 1, 55–61.

Kitahara, S., 1960. The solubility of quartz in aqueous sodium chloride solutions at high temperatures and high pressures. Rev. Phys. Chem. Jpn. 30, 115–121.

Kojitani, H., Akaogi, M., 1994. Calorimetric study of olivine solid solutions in the system Mg_2SiO_4. Phys. Chem. Miner. 20, 536–540.

Kuma, K., Suzuki, Y., Matsunaga, K., 1993. Solubility and dissolution rate of colloidal γ-FeOOH in seawater. Water Resour. 27, 651–657.

Kuyunko, N.S., Malinin, S.D., Khodakovskiy, I.L., 1983. An experimental study of aluminium ion hydrolysis at 150, 200, and 250°C. Geochem. Int. 20, 76–86.

Lee, H.Y., Ganguly, J., 1988. Equilibrium composition of coexisting garnet and orthopyroxene: experimental determinations in the system FeO–MgO–Al_2O_3–SiO_2 and applications. J. Petrol. 29, 93–113.

Lengweiler, H., Buser, W., Feitknecht, W., 1961a. Die Ermittlung der Löslichkeit von Eisen (III)-Hydroxiden mit ^{59}Fe: I. Fallungs- und Auflösungsversuche. Helv. Chim. Acta 44, 796–804.

Lengweiler, H., Buser, W., Feitknecht, W., 1961b. Die Ermittlung der Löslichkeit von Eisen (III)-Hydroxiden mit ^{59}Fe: II. Der Zustand kleinster Mengen Eisen (III)-hydroxid in wässeriger Lösnung. Helv. Chim. Acta 44, 805–811.

Liberti, A., Chintella, C., Corigliano, F., 1963. Mononuclear hydrolysis of titanium(IV) from partition equilibria. J. Inorg. Nucl. Chem. 25, 415–427.

Mackenzie, F.T., Gees, R., 1971. Quartz: synthesis at earth surface conditions. Science 173, 533–535.

McCallister, R.H., Finger, L.W., Ohashi, Y., 1976. Intracrystalline Fe^{2+}–Mg^{2+} equilibria in three natural Ca-rich clinopyroxenes. Am. Mineral. 61, 671–676.

Morey, G.W., Hesselgesser, J.M., 1951. The solubility of quartz and some other substances in superheated steam at high pressures. Am. Soc. Mech. Engl. Trans. 73, 868–875.

Morey, G.W., Fournier, R.O., Rowe, J.J., 1962. The solubility of quartz in water in the temperature interval from 25 to 300°. Geochim. Cosmochim. Acta 26, 1029–1043.

Newton, R.C., Charlu, T.V., Kleppa, O.J., 1980. Thermochemistry of the high structural state plagioclases. Geochim. Cosmochim. Acta 44, 933–942.

O'Neill, H.S.C., Navrotsky, A., 1983. Simple spinels: crystallographic parameters, cation radii, lattice energies, and cation distribution. Am. Mineral. 68, 181–194.

O'Neill, H.S.C., Navrotsky, A., 1984. Cation distribution and

thermodynamic properties of binary spinel solid solutions. Am. Mineral. 69, 733–753.

Ottonello, G., Princiavalle, F., Della Giusta, A., 1990. Temperature, compositions, and f_{O_2} effects on intersite distribution of Mg and Fe^{2+} in olivines: experimental evidence and theoretical interpretation. Phys. Chem. Miner. 17, 301–312.

Pokrovskii, V.A., Helgeson, H.C., 1995. Thermodynamic properties of aqueous species and the solubilities of minerals at high pressures and temperatures: the system Al_2O_3–H_2O–NaCl. Am. J. Sci. 295, 1255–1342.

Rimstidt, J.D., 1997. Quartz solubility at low temperatures. Geochim. Cosmochim. Acta 61, 2553–2558.

Robie, R.A., Hemingway, B.S., 1995. Thermodynamic properties of minerals and related substances at 298.15 K and 1 bar (105 Pascals) pressures and at higher temperatures. U.S. Geol. Surv. Bull. 2131, 461 pp.

Sack, R.O., 1980. Some constrains on the thermodynamic mixing properties of Fe–Mg orthopyroxenes and olivines. Contrib. Mineral. Petrol. 71, 257–269.

Sack, R.O., 1982. Spinels as petrogenetic indicators: activity–composition relations at low pressures. Contrib. Mineral. Petrol. 79, 169–182.

Sack, R.O., Ghiorso, M.S., 1989. Importance of considerations of mixing properties in establishing an internally consistent thermodynamic database: thermochemistry of minerals in the system Mg_2SiO_4–Fe_2SiO_4–SiO_2. Contrib. Mineral. Petrol. 102, 41–68.

Sack, R.O., Ghiorso, M.S., 1991. An internally consistent model for the thermodynamic properties of Fe–Mg-titanomagnetite–aluminate spinels. Contrib. Mineral. Petrol. 106, 474–505.

Sack, R.O., Ghiorso, M.S., 1994a. Thermodynamics of multicomponent pyroxenes: I. Formulation of a general model. Contrib. Mineral. Petrol. 116, 277–286.

Sack, R.O., Ghiorso, M.S., 1994b. Thermodynamics of multicomponent pyroxenes: II. Phase relations in the quadrilateral. Contrib. Mineral. Petrol. 116, 287–300.

Saxena, S.K., 1981. The MgO–Al_2O_3–SiO_2 system: free energy of pyrope and Al_2O_3-enstatite. Geochim. Cosmochim. Acta 45, 821–825.

Saxena, S.K., Ghose, S., 1971. Mg^{2+}–Fe^{2+} order–disorder and the thermodynamics of the orthopyroxene solution. Am. Mineral. 56, 532–559.

Saxena, S.K., Ghose, S., Turnock, A.C., 1974. Cation distribution in low-calcium pyroxenes: dependence on temperature and calcium content and the thermal history of lunar and terrestrial pigeonite. Earth Planet. Sci. Lett. 21, 194–200.

Sergeyeva, E.I., Suleimenov, O.M., Khodakovsky, I.L., 1988. Investigation of hematite (Fe_2O_3) solubility under hydrothermal conditions. Terra Cognita 8, 182.

Shock, E.L., Helgeson, H.C., 1988. Calculation of the thermodynamic an transport properties of aqueous species at high pressures and temperatures: correlation algorithms for ionic species and equation of state predictions to 5 kb and 1000°C. Geochim. Cosmochim. Acta 53, 2009–2036.

Shock, E.L., Helgeson, H.C., Sverjensky, D.A., 1989. Calculations of the thermodynamic and transport properties of aqueous species at high pressures and temperatures: standard partial molal properties of inorganic neutral species. Geochim. Cosmochim. Acta 53, 2157–2183.

Shock, E.L., Oelkers, E.H., Johnson, J.W., Sverjensky, D.A., Helgeson, H.C., 1992. Calculation of the thermodynamic properties of aqueous species at high pressures and temperatures: effective electrostatic radii, dissociation constants, and standard partial molal properties to 1000°C and 5 kbar. J. Chem. Soc., Faraday Trans. 88, 803–826.

Shock, E.L., Sassani, D.C., Willis, M., Sverjensky, D.A., 1997. Inorganic species in geologic fluids: correlations among standard molal thermodynamic properties of aqueous ions and hydroxide complexes. Geochim. Cosmochim. Acta 61, 907–950.

Siever, R., 1962. Silica solubility 0–200°C, and the diagenesis of siliceous sediments. J. Geol. 70, 127–150.

Spencer, K.J., Lindsley, D.H., 1981. A solution model for coexisting iron–titanium oxides. Am. Mineral. 66, 1189–1201.

Stefánsson, A., Gíslason, S.R., Arnórsson, S., 2000. Dissolution of primary minerals of basalt in natural waters: II. Mineral saturation state. Chem. Geol. in press.

Tanger, J.C., Helgeson, H.C., 1988. Calculation of the thermodynamic and transport properties of aqueous species at high pressures and temperatures. Am. J. Sci. 288, 19–98.

Torgeson, D.R., Sahama, T.G., 1948. A hydrofluoric acid solution calorimeter and the determination of the heats of formation of Mg_2SiO_4, $MgSiO_3$, and $CaSiO_3$. J. Am. Chem. Soc. 70, 2156–2160.

Trestman-Matts, A., Dorris, S.E., Kumarakrishnan, S., Mason, T.O., 1983. Thermoelectric determination of cation distribution in Fe_3O_4–Fe_2TiO_4. J. Am. Ceram. Soc. 66, 829–834.

Van Lier, J.A., de Bruyn, P.L., Overbeek, J.T.G., 1960. The solubility of quartz. J. Phys. Chem. 64, 1675–1682.

Verdes, G., Gout, R., Castet, S., 1992. Thermodynamic properties of the aluminate ion and of bayerite, boehmite, diaspore and gibbsite. Eur. J. Miner. 4, 767–792.

von Seckendorff, V., O'Neill, H.S.C., 1993. An experimental study of Fe–Mg partitioning between olivine and orthopyroxene at 1173, 1273 and 1473 K and 1.6 GPa. Contrib. Mineral. Petrol. 113, 196–207.

Weill, D.F., Fyfe, W.S., 1964. The solubility of quartz in H_2O in the range 1000–4000 bars and 400–500°C. Geochim. Cosmochim. Acta 28, 1243–1255.

Wesolowski, D.J., 1992. Aluminium speciation and equilibria in aqueous solution: I. The solubility of gibbsite in the system Na–K–Cl–OH–$Al(OH)_4$ from 0 to 100°C. Geochim. Cosmochim. Acta 56, 1065–1091.

Wiser, N.M., Wood, B.J., 1991. Experimental determination of activities in Fe–Mg olivine at 1400 K. Contrib. Mineral. Petrol. 108, 146–153.

Wood, B.J., Kleppa, O.J., 1981. Thermochemistry of forsterite–fayalite olivine solutions. Geochim. Cosmochim. Acta 45, 534–539.

Wu, C.C., Mason, T.O., 1981. Thermopower measurement of

cation distribution in magnetite. J. Am. Ceram. Soc. 64, 520–552.

Yishan, Z., Ruiying, A., Chen, Y., 1986. Determination of the solubility of Fe_2O_3 in dilute aqueous solutions at 300°C and 10 MPa. Sci. Sin. B 29, 1221–1232.

Ziemniak, S.E., Jones, M.E., Combs, K.E.S., 1993. Solubility behaviour of titanium(IV) oxide in alkaline media at elevated temperatures. J. Sol. Chem. 22, 601–623.

Ziemniak, S.E., Jones, M.E., Combs, K.E.S., 1995. Magnetite solubility and phase stability in alkaline media at elevated temepratures. J. Sol. Chem. 24, 837–877.